International Journal of Nanomedicine

Dovepress
open access to scientific and medical research

Open Access Full Text Article

ORIGINAL RESEARCH

Preparation and in vivo evaluation of a topical hydrogel system incorporating highly skin-permeable growth factors, quercetin, and oxygen carriers for enhanced diabetic wound-healing therapy

This article was published in the following Dove Press journal:
International Journal of Nanomedicine

Jun-Pil Jee[1,*]
Rudra Pangeni[2,*]
Saurav Kumar Jha[2]
Youngro Byun[3]
Jin Woo Park[2]

[1]College of Pharmacy, Chosun University, Gwangju 61452, Republic of Korea; [2]College of Pharmacy and Natural Medicine Research Institute, Mokpo National University, Muan-gun, Jeonnam 58554, Republic of Korea; [3]Department of Molecular Medicine and Biopharmaceutical Science, Graduate School of Convergence Science and Technology, College of Pharmacy, Seoul National University, Seoul 08826, Republic of Korea

*These authors contributed equally to this work

Correspondence: Youngro Byun
Department of Molecular Medicine and Biopharmaceutical Science, Graduate School of Convergence Science and Technology, College of Pharmacy, Seoul National University, 1 Gwanak-ro, Seoul 08826, Republic of Korea
Tel +82 2 880 7866
Fax +82 2 872 7864
Email yrbyun@snu.ac.kr

Jin Woo Park
College of Pharmacy and Natural Medicine Research Institute, Mokpo National University, 1666 Youngsan-ro, Muan-gun, Jeonnam 58554, Republic of Korea
Tel +82 61 450 2704
Fax +82 61 450 2689
Email jwpark@mokpo.ac.kr

Purpose: We created and evaluated an enhanced topical delivery system featuring a combination of highly skin-permeable growth factors (GFs), quercetin (QCN), and oxygen; these synergistically accelerated re-epithelialization and granulation tissue formation of/in diabetic wounds by increasing the levels of GFs and antioxidants, and the oxygen partial pressure, at the wound site.

Methods: To enhance the therapeutic effects of exogenous administration of GFs for the treatment of diabetic wounds, we prepared highly skin-permeable GF complexes comprised of epidermal growth factor (EGF), insulin-like growth factor-I (IGF-I), platelet-derived growth factor-A (PDGF-A), and basic fibroblast growth factor (bFGF), genetically attached, via the N-termini, to a low-molecular-weight protamine (LMWP) to form LMWP-EGF, LMWP-IGF-I, LMWP-PDGF-A, and LMWP-bFGF, respectively. Furthermore, quercetin (QCN)- and oxygen-carrying 1-bromoperfluorooctane (PFOB)-loaded nanoemulsions (QCN-NE and OXY-PFOB-NE) were developed to improve the topical delivery of QCN and oxygen, respectively. After confirming the enhanced penetration of LMWP-GFs, QCN-NE, and oxygen delivered from OXY-PFOB-NE across human epidermis, we evaluated the effects of combining LMWP-GFs, QCN-NE, and OXY-PFOB-NE on proliferation of keratinocytes and fibroblasts, and the chronic wound closure rate of a diabetic mouse model.

Results: The optimal ratios of LMWP-EGF, LMWP-IGF-I, LMWP-PDGF-A, LMWP-bFGF, QCN-NE, and OXY-PFOB-NE were 1, 1, 0.02, 0.02, 0.2, and 60, respectively. Moreover, a Carbopol hydrogel containing LMWP-GFs, QCN-NE, and OXY-PFOB-NE (LMWP-GFs/QCN-NE/OXY-PFOB-NE-GEL) significantly improved scratch-wound recovery of keratinocytes and fibroblasts in vitro compared to that afforded by hydrogels containing each component alone. LMWP-GFs/QCN-NE/OXY-PFOB-NE-GEL significantly accelerated wound-healing in a diabetic mouse model, decreasing wound size by 54 and 35% compared to the vehicle and LMWP-GFs, respectively.

Conclusion: LMWP-GFs/QCN-NE/OXY-PFOB-NE-GEL synergistically accelerated the healing of chronic wounds, exerting both rapid and prolonged effects.

Keywords: diabetic wound-healing, topical hydrogel, highly skin-permeable growth factors, quercetin, 1-bromoperfluorooctane, oxygen delivery

Introduction

Cutaneous wound repair is a complex and well-orchestrated dynamic process that consists of overlapping biochemical and physiological phenomena, including hemostasis/

coagulation, inflammation, proliferation, and tissue remodeling.[1] The process is driven by intercellular interactions among growth factors (GFs) and cytokines, which are secreted at the wound site by inflammatory cells and other stromal cells in response to tissue injury.[1,2] However, chronic wounds, such as diabetic foot ulcers (DFUs), venous leg ulcers, and pressure ulcers may fail to achieve complete re-epithelialization in the appropriate time-frame. These chronic wounds may show decreased collagen deposition and granulation tissue formation, which are associated with a reduction in endogenous GF levels or activity at the wound site.[2,3] Ulcers and wounds that are slow to heal represent a major burden for healthcare systems. This is particularly problematic in populations where the average age and incidence of diabetes are increasing.[4]

DFUs are among the most prevalent and severe complications experienced by patients with diabetes, and 15–25% of patients may have DFUs more than once in their lifetime.[5] These chronic and refractory ulcers are associated with peripheral neuropathy, impaired vascular function and angiogenesis, decreased collagen production, or chronic inflammation, as a result of long-term hyperglycemia.[6,7] Furthermore, chronic wounds are characterized by elevated levels of proinflammatory cytokines, proteases, reactive oxygen species (ROS), and senescent cells with impaired proliferative and secretory capacities.[8] This means that they do not respond to typical wound healing signals, and are prone to persistent infections and a deficiency of stem cells, which are also often dysfunctional. Recently, advanced therapies have been used to treat chronic wounds that do not respond to standard care. These include negative-pressure wound therapy, hyperbaric oxygen therapy, biological and bioengineered therapies employing platelet-rich plasma or GFs, biophysical modalities (electrical stimulation and ultrasound), placement of acellular matrix tissues, and bioengineering and stem cell therapies.[9–12]

Impaired chronic wound healing is associated with decreased secretion of endogenous GFs. Therefore, providing exogenous GFs at precisely timed intervals would stimulate faster re-epithelialization, as well as reduce the risk of infection.[13,14] To date, GFs such as epidermal growth factor (EGF), transforming growth factor beta (TGF-β), fibroblast growth factor (FGF), platelet-derived growth factor (PDGF), insulin-like growth factor (IGF), vascular endothelial cell GF, and keratinocyte GF-2 have been considered key regulators of the wound healing process.[15] These GFs have been studied with respect to whether they can promote neovascularization, re-epithelialization and collagen deposition, and thus stimulate wound repair by inducing proliferation of endothelial cells and fibroblasts/keratinocytes at sites where healing is impaired.[16] However, few therapies that use PDGF, EGF, or FGF are commercially available or have successfully completed clinical trials for diabetic wound care.[17] The reasons for this are as follows: a single GF is often insufficient to promote wound closure in diabetic ulcers because a specific set of cytokines and/or GFs is required to interact with receptors, other GFs, and extracellular matrix (ECM) components at target sites; the stratum corneum (SC) on the outermost skin forms a strong barrier to topically applied GFs; low GF concentrations are present in chronic ulcer wounds due to their rapid exudation from and/or dilution in the wound bed; and short GF half-life and loss of bioactivity caused by enzymatic degradation and inactivation due to elevated levels of matrix metalloproteinase (MMP) activity in the wound bed.[18–21] Consequently, efforts have been made to overcome these limitations and develop efficient topical delivery systems. These include poly(ether) urethane-polydimethylsiloxane/fibrin-based scaffolds, nanofibers, hydrogels fabricated with ECM components such as collagen and hyaluronic acid, poly(lactic-co-glycolic acid) micro-particulate systems, biocompatible wound dressings using chitosan, and colloidal systems that incorporate heparin and vitronectin to improve their healing capacity by maintaining high concentrations of GFs at the wound site.[22–25] In our previous studies, we designed rapid and enhanced skin-permeable EGF, IGF-I, PDGF-A, and basic fibroblast growth factor (bFGF) by genetically fusing a positively charged low-molecular-weight protamine (LMWP) to N-termini to form LMWP-EGF, LMWP-IGF-I, LMWP-PDGF-A, and LMWP-bFGF, respectively. These molecules had markedly increased in vitro skin infiltration, resulting in significantly accelerated recovery from acute and diabetic full-thickness wounds compared to native GFs.[26,27]

In chronic wounds, the hypoxic and inflammatory environment increases ROS production, which damages ECM proteins and by extension causes cell damage, leading to stimulation of proteases and inflammatory cytokines.[28,29] Therefore, applying strong antioxidants may reduce ROS to normal levels, preventing wounds from becoming chronic.[30] Quercetin (2-(3,4-dihydroxyphenyl)-3,5,7-trihydroxy-4H-chromen-4-one; QCN) is a naturally occurring flavonoid found in vegetables, tea, and berries. It has anti-ulcer, -inflammatory, and -infective activities due to its ability to scavenge oxygen free-radicals and inhibit lipid peroxidation.[31] Therefore, QCN is a promising topical healing agent because it can increase fibroblast proliferation, decrease immune cell infiltration, and adjust activity in fibrosis-associated signaling pathways.[32] However, it has a very limited ability to penetrate

the skin; although it is insoluble in water and has a favorable lipophilic partition coefficient (1.82±0.32) due to the nonpolar groups in its structure, the polar hydroxyl groups hinder skin penetration.[33] Therefore, to deliver sustained QCN at therapeutic levels, a suitable carrier (eg, a nanoemulsion [NE]) must be used to ensure a high loading capacity and adherence to the skin.[32]

Tissue repair requires increased metabolic activity, resulting in a high demand for oxygen.[34] In addition, the oxygen partial pressure in chronic diabetic ulcers is <5 mmHg, which is six- to eight-fold lower than normal subcutaneous levels.[35,36] Therefore, wound healing is delayed under hypoxic conditions, and increased oxygen tension in a wound promotes healing by stimulating phagocytosis, degradation of necrotic wound tissue, collagen production, neovascularization, and neutrophil-mediated antimicrobial activity.[37] Recently, various treatments have been used to increase oxygen supply to wounds and accelerate repair. However, hyperbaric oxygen is not always practical or readily available.[38] An alternative strategy is to use topical oxygen therapies that involve oxygen carriers, such as perfluorocarbons (PFCs). The oxygen solubility of PFCs is approximately 20-fold greater than that of water and they contain a nonreactive moiety.[36,39] However, because they are hydrophobic, PFCs must be emulsified or formulated as colloidal suspensions to allow them to deliver sufficient oxygen deep into a wound for several hours and accelerate local tissue repair.[36,39,40]

In this study, we hypothesized that a combined treatment of LMWP-fused GFs (LMWP-GFs) that included LMWP-EGF, LMWP-IGF-I, LMWP-PDGF-A, and LMWP-IGF-I would considerably accelerate diabetic wound healing, re-epithelialization, and dermal-tissue remodeling by minimizing exudation. These benefits would be due to enhanced skin penetration and the synergistic effects of combining the GFs. Furthermore, combining the LMWP-GFs with QCN and oxygen might synergistically accelerate wound closure, especially in the early stages of diabetic ulcer wounds, due to the activation of fibroblasts. To demonstrate this, we developed a QCN-loaded oil-in-water (o/w) nanoemulsion (QCN-NE) and a hyperoxygenated NE by encapsulating 1-bromoperfluorooctane (PFOB) with phosphatidylcholine (OXY-PFOB-NE) to enhance the epidermal delivery and skin retention of QCN oxygen to wounds. We determined the optimal concentration ratios of LMWP-EGF, LMWP-IGF-I, LMWP-PDGF-A, LMWP-bFGF, QCN, and OXY-PFOB-NE for synergistic effects on the proliferation of keratinocytes and fibroblasts, and for collagen synthesis. In addition, we confirmed enhanced skin infiltration and human epidermal drug retention after incorporating LMWP-GFs, QCN-NE, and OXY-PFOB-NE into a Carbopol hydrogel matrix (LMWP-GFs/QCN-NE/OXY-PFOB-NE-GEL). Finally, we showed that LMWP-GFs/QCN-NE/OXY-PFOB-NE-GEL synergistically enhanced the rate of recovery from scratch wounds in vitro, and accelerated chronic wound closure by stimulating re-epithelialization and regenerating connective tissue in a diabetic mouse model.

Materials and methods

Materials

Recombinant human EGF, IGF-I, PDGF-A, bFGF, LMWP-EGF, LMWP-IGF-I, LMWP-PDGF-A, and LMWP-bFGF were obtained from BIO FD&C (Jeonnam, Republic of Korea). QCN (purity >95%), polyethylene glycol 400 (PEG 400), polyoxyethylene (20) sorbitan monolaurate (Tween 20), and polyoxyethylene (80) sorbitan monolaurate (Tween 80) were obtained from Merck KGaA (Darmstadt, Germany). Caprylocaproyl macrogol-8-glycerides (Labrasol) and oleoyl polyoxylglycerides (Labrafil M 1944 CS) were provided by Gattefossé (Saint Priest, France). Polyethoxylated castor oil (Cremophor EL) was obtained from BASF (Ludwigshafen, Germany). 1-Bromoperfluorooctane (PFOB) was purchased from Synquest Laboratories (Alachua, FL, USA). Soy phosphatidylcholine was kindly donated by Lipoid GmbH (Ludwigshafen, Germany). Carbopol 981 was the product of Lubrizol Corporation (Wickliffe, OH, USA). Human keratinocytes (ATCC® CRL-2404™, HaCaT) and fibroblasts (ATCC® CRL-1947™, CCD-986sk) were purchased from the American Type Culture Collection (ATCC, University Boulevard, VA, USA). Dermatomed, human, cadaveric full-thickness skin and epidermis (3×3 cm^2) from the backs and thighs of Caucasians were purchased from a skin and tissue bank (HansBiomed Corp.; Daejeon, Republic of Korea). Each material was frozen in 10% (v/v) glycerol solution by the supplier and stored at −70°C prior to experiments. All studies using research materials that have been separated and processed from human derivatives so that the human body cannot be directly harvested and used by the general public are not required to submit documentation or approval from a formally constituted review board or ethics committee (Article 33, Enforcement Rule of the Bioethics and Safety Act in the Republic of Korea).

Animals

C57BL/6 mice (females, 20–25 g) were purchased from Orientbio (Gwangju, Republic of Korea). Ethical approval

for this study was obtained from the Institutional Animal Care and Use Committee (IACUC) of Mokpo National University (Jeonnam, Republic of Korea). All animal experiments were performed in accordance with the National Institutes of Health Guidelines for the Care and Use of Laboratory Animals and the IACUC guidelines.

Preparation and characterization of LMWP-GFs

LMWP-fused EGF, IGF-I, PDGF-A, and bFGF were obtained as described previously.[26,41,42] Briefly, LMWP-EGF, LMWP-IGF-I, LMWP-PDGF-A, and LMWP-bFGF cDNAs were prepared by concatenating the LMWP codons onto the EGF, IGF-I, PDGF-A, and bFGF genes using serial polymerase chain reaction (PCR). Next, the cDNAs were inserted between *Nde* I and *Xho* I restriction sites by sub-cloning them into a TOPO vector, followed by PCR amplification using 5′–GTGAGCCGTAGACGTAGACGTAGAGGTGGTCGTAGACGTAGAAATAGTGACTCTGAA–3′, 5′–GTGAGCCGTAGACGTAGACGTAGAGGTGGTCGTAGACGTAGAGGACCGGAGACGCTC–3′, 5′–GTGAGCCGTAGACGTAGACGTAGAGGTGGTCGTAGACGTAGAAGCATCGAGGAAGCT–3′, and 5′–GTGAGCCGTAGACGTAGACGTAGAGGTGGTCGTAGACGTAGACCCGCCTTGCCCGAG–3′ as the forward primers, and 5′–ATGATGATGATGATGATGGCGCAGTTCCCACCA–3′, 5′–ATGATGATGATGATGATGAGCTGACTTGGCAGG–3′, 5′–ATGATGATGATGATGATGTTAGGTGGGTTTTAA–3′, and 5′–ATGATGATGATGATGATGGCTCTTAGCAGACAT–3′ as the reverse primers for LMWP-EGF, LMWP-IGF-I, LMWP-PDGF-A, and LMWP-bFGF, respectively. Each PCR product was ligated into a pET-41b(+) expression vector that had been digested with *Nde* I/*Xho* I, and the resulting plasmids were transformed into *E. coli* cells (BL21-DE3). When the optical density at 600 nm of lysogeny broth medium reached 0.6–0.8, all of the LMWP-GFs were expressed by adding 1 mM isopropyl-β-D-thiogalactopyranoside (IPTG) and cultured overnight at 25°C. Thereafter, the cells were harvested by centrifugation at 6,000×g for 10 min at 4°C and resuspended in cell lysis buffer (1% sodium lauroyl sarcosinate in phosphate-buffered saline [PBS, pH 7.5] containing 10 mM NaCl) with sonication. The supernatant containing each LMWP-GF was collected after further centrifugation (12,000×g, 10 min, 4°C) and purified using His-Tag affinity chromatography on a Ni-charged resin, as well as a Sephadex G-100 column by eluting with imidazole-containing PBS (pH 7.5) and 20 mM PBS (pH 7.5) containing 500 mM NaCl, respectively. The purified LMWP-GFs were quantified using sodium dodecyl sulfate-polyacrylamide gel electrophoresis (SDS-PAGE) with Coomassie blue staining and their intact molecular weights were determined by liquid chromatography-electrospray ionization-tandem mass spectrometry (LC-ESI-MS; Orbitrap LC-MS; Thermo Fisher Scientific, Waltham, MA, USA). The sequences of the LMWPs appended to the N-termini of the purified LMWP-EGF, LMWP-IGF-I, LMWP-PDGF-A, and LMWP-bFGF were confirmed using an Applied Biosystems Procise 491 protein sequencer (Courtaboeuf, France).

In vitro human skin penetration of LMWP-GFs

To demonstrate that the LMWP-GFs showed enhanced skin penetration, in vitro human skin permeability assays were performed using the Franz diffusion cell system (Labfine, Gyeonggi-do, Republic of Korea). Excised full-thickness human skin was mounted with the SC facing upward on the receptor phase compartment of a Franz diffusion cell system, which was then filled with 5 mL PBS (pH 7.4). Next, the donor compartment was clamped in place (the diffusion area was 0.785 cm^2) and the cells were allowed to equilibrate for at least 60 min to confirm the integrity of the skin. After reaching an equilibrium, the donor compartment was loaded with 300 μL of 0.1% (w/w) Carbopol hydrogel containing each fluorescent dye (AlexaFluor 647)-labeled EGF (50 μg/mL), IGF-I (50 μg/mL), PDGF-A (50 μg/mL), bFGF (50 μg/mL), LMWP-EGF (50 μg/mL), LMWP-IGF-I (50 μg/mL), LMWP-PDGF-A (50 μg/mL), or LMWP-bFGF (50 μg/mL). At 12 h after loading, the diffusion cell was disassembled and the skin was carefully removed and washed twice with deionized water. The washed skin was retained in solution, frozen, and sliced vertically into 10 μm sections using a cryo-microtome (Leica CM 1850; Leica Microsystems, Bannockburn, IL, USA). The cross-sections were imaged at 647 nm using confocal laser scanning microscopy (Carl Zeiss, Oberkochen, Germany).

Preparation and characterization of QCN-NE and OXY-PFOB-NE

A low-energy spontaneous emulsification method was used to prepare QCN-NE, as described previously.[43] The solubility and miscibility of QCN in various oils, surfactants, and co-surfactants were used to select the NE components. Then, pseudo-ternary phase diagrams were constructed by aqueous phase titration using combinations of Capryol 90 and Labrafil

M 1944 CS (1:1, w/w) as the oil phase, Labrasol and Tween 80 (1:1, w/w) as surfactants, Cremophor EL and PEG 400 (1:1, w/w) as co-surfactants, and water at room temperature. Next, a mixture of surfactants and co-surfactants (S_{mix}) was blended in various weight ratios (3:1 to 1:3) using increasing concentrations of co-surfactant relative to surfactant. Thereafter, pseudoternary phase diagrams were prepared at different weight ratios of oil to S_{mix} (1:9 to 9:1) by the slow addition of water. In the pseudo-ternary diagrams, the o/w NE was identified visually as the region where clear and transparent droplets were obtained. The optimum composition for the o/w NE selected from the clear zone of pseudo-ternary phase diagrams was 22.2% oil phase (Capryol 90: Labrafil M 1944 CS, 1:1, w/w), 33.3% surfactants (Labrasol: Tween 80, 1:1, w/w), 11.1% co-surfactants (Cremophor EL: PEG 400, 1:1, w/w), and 33.4% aqueous phase. Here, QCN was maximally solubilized and there was no precipitation or phase separation when it was infinitely diluted with water. To prepare the QCN-NE, 1.2 mg of QCN dissolved in 400 mg of oil phase was added to 800 mg of S_{mix} (3:1, w/w) and water was added dropwise to the mixture with continuous mixing.

PFOB-NE was prepared using high pressure homogenization. In brief, soy phosphatidylcholine and Tween 80 were dissolved in PBS (pH 7.4) and stirred using a magnetic stirrer for 30 min at room temperature. PFOB was then added to the mixture and stirred for 30 min. The final composition of the PFOB emulsion was 1.875% (w/v) soy phosphatidylcholine, 0.625% (w/v) Tween 80, 50% (w/v) PFOB, and 47.5% (w/v) PBS (pH 7.4). The mixture was homogenized in a high speed homogenizer (HG-15A; Daihan Scientific Co., Ltd., Wonju, Republic of Korea) at 8,100 rpm for 30 s to obtain a crude emulsion and then treated for 5 cycles at 15,000 psi in a LV1-30K microfluidizer (Microfluidics, Westwood, MA, USA). The PFOB-NE obtained was stored at 4°C for further study. Next, the different concentrations of PFOB-NE were prepared by diluting the stock 50% (w/v) PFOB-NE solution with PBS (pH 7.4). Oxygen was bubbled into 5 mL of PFOB-NE at a rate of 1 mL/min. In addition, oxygen released from the OXY-PFOB-NE was quantified by collecting it in a CO_2 incubator (37°C, 5% CO_2). The concentration of oxygen in the OXY-PFOB-NE was analyzed at predetermined time intervals (0, 1, 2, 3, 6, 12, 24, and 36 h). Oxygen bubbled into PBS (pH 7.4) (OXY-PBS) was treated using the same method to provide a control. The oxygen concentration was analyzed using a NeoFox fluorometer equipped with a Fospor-R oxygen sensor (OceanOptics, Dunedin, FL, USA). A two-point calibration was performed each day using CO_2 gas (0% O_2) and air (20.9% O_2).

The mean droplet size, polydispersity indexes (PDIs), and zeta potential of the optimized formulations for QCN-NE and OXY-PFOB-NE were determined using a dynamic laser light scattering analyzer (Zetasizer Nano ZS90; Malvern Instruments, Malvern, UK) at 25°C after dilution with deionized water (1:20). In addition, the QCN-NE and OXY-PFOB-NE were examined using transmission electron microscopy (TEM). A drop of QCN-NE or OXY-PFOB-NE diluted 100-fold was placed on a copper grid and the excess fluid was removed with filter paper. The samples were stained with a 2% (w/v) aqueous solution of phosphotungstic acid and the excess was removed after 1 min. The dried samples were examined using TEM (JEM-200; JEOL, Tokyo, Japan).

Preparation of topical hydrogel containing LMWP-GFs, QCN-NE, and OXY-PFOB-NE

To formulate the hydrogel containing the LMWP-GFs, QCN-NE, and OXY-PFOB-NE, 20 µL of QCN-NE (containing 1 mg/mL of QCN) was mixed with deionized water (80 µL) and stirred continuously. Then, an aqueous solution of LMWP-GFs comprising 200 µL LMWP-EGF (500 µg/mL), 200 µL LMWP-IGF-I (500 µg/mL), 10 µL LMWP-PDGF-A (200 µg/mL), and 10 µL LMWP-bFGF (200 µg/mL), as well as 20 µL of OXY-PFOB-NE (300 mg/mL PFOB-NE), was added to the QCN-NE and gently vortex mixed. Carbopol (0.1 g) and PEG 400 (10 g) were dissolved in deionized water (89.9 g) with constant stirring to form a transparent Carbopol gel (0.2%, w/w). After adjusting the Carbopol gel to pH 6.0 with triethanolamine (50%, w/w), the mixture of LMWP-GFs, QCN-NE, and OXY-PFOB-NE was added to 460 µL of Carbopol hydrogel (0.2%, w/w) and saturated for 10 min with 100% oxygen gas to obtain the LMWP-GFs, QCN-NE, and OXY-PFOB-NE-loaded hydrogel (LMWP-GFs/QCN-NE/OXY-FPOB-NE-GEL) (Figure 1). The concentration of each of the active components in the final hydrogel was based on the optimal effects observed in the in vitro cell proliferation and procollagen synthesis assays. The final concentrations in the hydrogel were 100 µg/mL LMWP-EGF, 100 µg/mL LMWP-IGF-I, 2 µg/mL LMWP-PDGF-A, 2 µg/mL LMWP-bFGF, 20 µg/mL QCN, and 6,000 µg/mL OXY-PFOB-NE.

After preparing LMWP-GFs/QCN-NE/OXY-FPOB-NE-GEL, the concentrations of each LMWP-GF and QCN in the hydrogel were assayed. A 0.5 mL sample of LMWP-GFs/

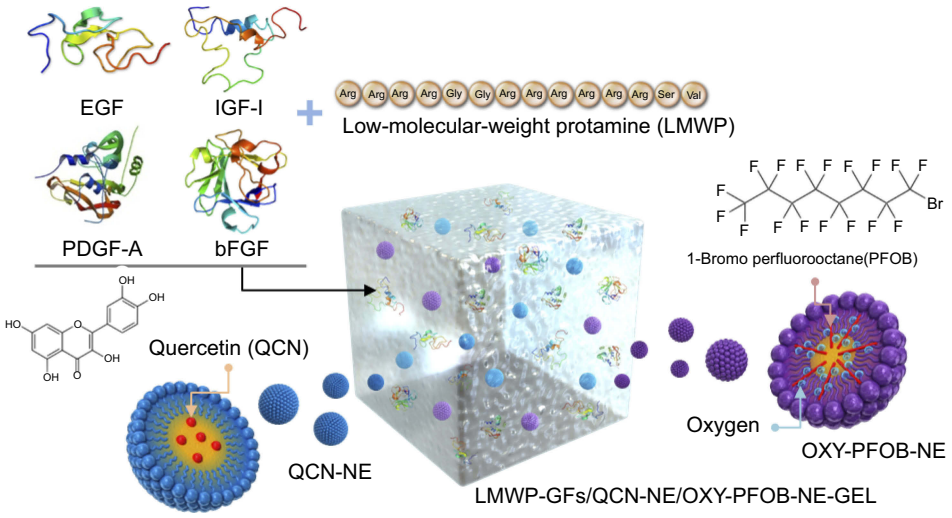

Figure 1 Schematic illustration of LMWP-GFs, QCN-NE, OXY-PFOB-NE, and a hydrogel comprising LMWP-GFs, QCN-NE, and OXY-PFOB-NE.
Abbreviations: LMWP, low-molecular-weight protamine; GFs, growth factors; LMWP-GFs, LMWP-fused GFs; QCN, quercetin; NE, nanoemulsion; QCN-NE, QCN-loaded NE; PFOB, 1-bromoperfluorooctane; OXY-PFOB-NE, oxygen-carrying PFOB-loaded NE.

QCN-NE/OXY-FPOB-NE-GEL was further diluted with 9.5 mL water and centrifuged at 18,000 rpm for 1 h at 4°C. The levels of all LMWP-GFs in aliquots of the supernatant were then analyzed via ELISA (absorbance at 450 nm) following the manufacturer's instructions (GenScript USA Inc., Piscataway, NJ, USA). To determine QCN levels, after removal of the remaining supernatants, the precipitates were dissolved in 0.5-mL amounts of methanol followed by filtration through a membrane 0.45 µm in pore size (polyvinylidene fluoride, PVDF). QCN concentrations were determined with the aid of a high-performance liquid chromatography (HPLC) system featuring a C18 column (4.6×150 mm, 5 µm, 100 Å, 20 µL sample injection) at 35°C; water with 2% (v/v) acetic acid (pH 2.6):acetonitrile (40:60, v/v) served as the mobile phase; the flow rate was 1 mL/min. QCN levels were measured by absorbance at 370 nm using a UV detector.

The average droplet sizes, PDIs, and zeta potentials of hydrogel QCN-NE and OXY-PFOB-NE were measured at 25°C via dynamic laser light scattering (Zetasizer Nano ZS90, Malvern Instruments), after dilution with deionized water (1:20). The morphologies of QCN-NE and OXY-PFOB-NE dispersed in the hydrogel were examined via TEM (JEM-200; JEOL) after negative staining with 2% (w/v) aqueous phosphotungstic acid, as described above.

Cell proliferation assays

The proliferation capacities of HaCaT and CCD-986sk cells used to evaluate the biological activities of the LMWP-GFs, QCN, and OXY-PFOB-NE were assessed. Briefly, HaCaT and CCD-986sk cells were seeded at a density of 5×10^3 cells/well and 1×10^4 cells/well, respectively, in 200 µL of Dulbecco's modified Eagle's medium (DMEM) containing 10% fetal bovine serum (FBS) and 1% penicillin/streptomycin in 96-well plates. Afterward, the HaCaT and CCD-986sk cells were cultured at 37°C in 95% air and 5% CO_2 for 24 h and 48 h, respectively. After overnight incubation in serum-free medium, the cells were treated for 24 h in low-serum medium (0.05% FBS) with LMWP-GFs comprising LMWP-EGF (500 ng/mL), LMWP-IGF-I (500 ng/mL), LMWP-PDGF-A (10 ng/mL), and LMWP-bFGF (10 ng/mL), QCN in 10% DMSO (0.1–25 µg/mL), and an aqueous dispersion of OXY-PFOB-NE (0.03–300 µg/mL PFOB-NE) alone or combined. Cell proliferation was assessed by adding 10 µL of WST-1 reagent to each well and incubating at 37°C for 1 h. Absorbance was measured at 450 nm using a multimode microplate reader (PerkinElmer, Waltham, MA, USA). The percentage of viable cells was calculated by comparing the values of treated cells to those of untreated cells for both the HaCaT and CCD-986sk cells.

Procollagen synthesis assay

To assess the combined effect of the LMWP-GFs (LMWP-EGF [500 ng/mL], LMWP-IGF-I [500 ng/mL], LMWP-PDGF-A [10 ng/mL], and LMWP-bFGF [10 ng/mL]), QCN in 10% DMSO (0.1 µg/mL), and an aqueous dispersion of OXY-PFOB-NE (30 µg/mL PFOB-NE) on

collagen synthesis, the biosynthesis of type I C-peptide from fibroblasts was used as a marker for procollagen secretion. Briefly, 5×10^3 CCD-986sk cells were seeded in 100 µL DMEM complete medium (10% FBS and 1% penicillin/streptomycin) in 96-well plates and cultured for 24 h. After the cells reached 80% confluence, the culture medium was removed and replaced with 100 µL sample solution prepared in DMEM containing 2.5% FBS and incubated for 24 h at 37°C in 95% air and 5% CO_2. Next, the culture supernatants were collected from each well and the level of procollagen type I C-peptide was determined using an enzyme-linked immunosorbent assay (ELISA) kit (Takara Bio, Shiga, Japan), in accordance with the manufacturer's instructions.

In vitro infiltration across a human epidermis

To compare the permeability of a hydrogel containing each native or LMWP-GF, the in vitro human epidermal permeability study was performed using the Franz diffusion cell system. Skin infiltration of QCN dispersed in 0.3% (w/v) sodium carboxymethyl cellulose (NaCMC) or QCN-NE incorporated in the 0.1% (w/w) Carbopol hydrogel, and un-oxygenized PFOB-NE or OXY-PFOB-NE dispersed in 0.1% (w/w) Carbopol hydrogel were also evaluated. After filling the receiver compartment with 5 mL PBS (pH 7.4), the donor compartment was loaded with 300 µL of hydrogel containing each native GF (EGF [100 µg/mL], IGF-I [100 µg/mL], PDGF-A [100 µg/mL], or bFGF [100 µg/mL]) or LMWP-GF (LMWP-EGF [100 µg/mL], LMWP-IGF-I [100 ng/mL], LMWP-PDGF-A [100 µg/mL], or LMWP-bFGF [100 µg/mL]). Similarly, 500 µL of QCN dispersed in 0.3% (w/v) NaCMC (1 mg/mL QCN) or QCN-NE dispersed in 0.1% (w/w) Carbopol hydrogel (1 mg/mL QCN) was loaded in the donor compartment. The receptor compartment filled with 5 mL of PBS (pH 7.4) containing 1% Tween 20 was stirred at 600 rpm and heated to maintain a skin surface temperature of 32°C throughout the experiment. Then, 200 µL of the receptor phase was withdrawn at 0, 1, 3, 6, 9, 12, and 24 h from each diffusion cell and replaced with the same volume of fresh PBS (pH 7.4). The withdrawn samples were passed through a membrane filter (pore size: 0.45 µm, PVDF) and stored at –20°C for analysis. The native and LMWP-GFs that infiltrated the epidermis were quantified via ELISA (absorbance at 450 nm) as directed by the manufacturer (GenScript USA Inc.). The levels of QCN that infiltrated the epidermis were determined using the HPLC system described above. To measure skin infiltration by oxygen from PFOB-NE, 500 µL of hydrogel containing un-oxygenized PFOB-NE (PFOB-NE-GEL; 300 µg/mL PFOB-NE) or OXY-PFOB-NE-GEL (300 µg/mL PFOB-NE) was loaded in the donor compartment and the oxygen level in the receptor compartment was monitored for up to 24 h using a NeoFox fluorometer equipped with a Fospor-R oxygen sensor (OceanOptics).

In vitro scratch-wound recovery assay

To investigate the wound healing efficacy of a hydrogel comprising LMWP-GFs, QCN-NE, and OXY-PFOB-NE, an in vitro scratch-wound recovery assay was performed. A total of 2.5×10^4 HaCaT or 4×10^4 CCD-986sk cells (in 200 µL DMEM with 10% [v/v] FBS and 1% [w/v] penicillin/streptomycin) was added to each well of a collagen-coated Essen ImageLock 96-well plate (Essen Bioscience, Ann Arbor, MI, USA), and incubated at 37°C for 48 h to produce confluent monolayers. Cell-free scratches 700–800-µm wide were created in the monolayers using a 96-pin IncuCyte wound-maker (Essen BioScience), and the detached cells were washed twice with PBS (pH 7.4). The HaCaT and CCD-986sk cells were further treated with 200 µL of hydrogel diluted with DMEM containing 0.5% FBS to apply LMWP-GFs (LMWP-EGF [500 ng/mL], LMWP-IGF-I [500 ng/mL], LMWP-PDGF-A [10 ng/mL], and LMWP-bFGF [10 ng/mL]), QCN-NE (equivalent to 0.1 µg/mL of QCN), and 30 µg/mL of OXY-PFOB-NE alone or combined. The plates with the HaCaT and CCD-986sk cells were incubated at 37°C in an IncuCyte FLR microscope (Essen Bioscience) for 12 h and 48 h, respectively, and wound recovery was quantified using IncuCyte FLR image analysis software, which detects cell edges and generates an overlay mask to calculate relative wound density.

In vivo diabetic wound healing efficacy

To evaluate the wound healing efficacy of the hydrogel containing LMWP-GFs, QCN-NE, and OXY-PFOB-NE, diabetes mellitus was induced in C57/BL6 mice by intraperitoneal streptozotocin (STZ) injections (50 mg/kg) for 5 consecutive days. Four weeks after STZ injection, blood glucose levels were measured using a glucometer (Roche Diabetes Care GmbH, Mannheim, Germany). Mice with blood glucose levels ≥250 mg/dL were considered diabetic and selected for study. For the full-thickness diabetic wound-healing study, mice were anesthetized with isoflurane (5%, v/v) and a full-thickness wound was created using an 8-mm biopsy punch at the center of the dorsal skin of each mouse. The wound area was sterilized with a povidone/iodine solution for 1 day, and the mice were then

randomly divided into five treatment groups, each of 24 mice. The initial wound areas (day 0 areas) were measured using a digital camera and ImageJ software (LOCI; University of Wisconsin, Madison, WI, USA). Each group was then treated topically once daily for 12 days with 30 µL amounts of control material (hydrogel only); LMWP-GFs-GEL (hydrogel containing LMWP-EGF [100 µg/mL], LMWP-IGF-I [100 µg/mL], LMWP-PDGF-A [2 µg/mL], and LMWP-bFGF [2 µg/mL]); QCN-NE-GEL (QCN-NE-dispersed hydrogel [20 µg/mL of QCN]); OXY-PFOB-NE-GEL (OXY-PFOB-NE-dispersed hydrogel [6,000 µg/mL PFOB-NE]); and LMWP-GFs/QCN-NE/OXY-PFOB-NE-GEL (hydrogel comprising LMWP-EGF [100 µg/mL], LMWP-IGF-I [100 µg/mL], LMWP-PDGF-A [2 µg/mL], LMWP-bFGF [2 µg/mL], QCN-NE [20 µg/mL QCN], and OXY-PFOB-NE [6,000 µg/mL]). In addition, identical full-thickness wounds of non-diabetic mice were treated topically with 30 µL amounts of hydrogel only (non-diabetic control), to allow comparison with normal wound-healing. Healing was evaluated by measuring the wound areas using a digital camera and ImageJ software (LOCI); the healing rate was expressed as a percentage of the remaining wound area.

To directly monitor and assess healing, three animals per group were sacrificed on each of days 3, 6, and 9 after treatment. The wounds and surrounding tissues were sampled using a biopsy punch prior to histological examination. The remaining 15 animals of each group were sacrificed on day 13. The excised wound tissues were immediately fixed in 10% (v/v) neutral phosphate-buffered formalin, routinely processed, and embedded in paraffin wax. The tissues embedded in paraffin wax were cut to a thickness of 6 µm and stained with hematoxylin and eosin (H&E) and Masson's trichrome (MT) to assess gross histopathological changes and assess collagen deposition in the wound area, respectively. Replicate sections were also stained immunohistochemically for cytokeratin 6 (CK6) to detect activated keratinocytes in the wound. Briefly, tissues were incubated overnight at 4°C with a polyclonal rabbit anti-CK6 primary antibody (PRB-169P; Covance, Princeton, NJ, USA), and then for 1 h with a secondary anti-rabbit horseradish peroxidase (HRP)-conjugated antibody (ab6802; Abcam, Cambridge, UK). To investigate α-smooth muscle actin (α-SMA) expression in wound-model specimens, the paraffin block was sectioned to a thickness of 3 µm and deparaffinized. For immunostaining, the tissue was incubated for 1 h at room temperature with a polyclonal rabbit anti-α-SMA primary antibody (1184-1; Epitomics, Burlingame, CA, USA) and then incubated for 10 min with a secondary anti-rabbit HRP-conjugated antibody (D39-15; Golden Bridge International, New York, NY, USA). Simultaneously stained sections were examined using light microscopy (BX-41; Olympus, Tokyo, Japan), and photomicrographs were recorded using an Olympus DP72 camera.

Statistical analysis

Unpaired data were evaluated using Student's *t*-test to compare two mean values, and one-way analysis of variance (ANOVA) followed by Tukey's multiple-comparison test was used to compare more than two mean values. All data were expressed as mean ± standard deviation. In all analyses, a *P*-value <0.05 was considered statistically significant.

Results and discussion

Characterization of LMWP-GFs

The purified LMWP-EGF, LMWP-IGF-I, LMWP-PDGF-A, and LMWP-bFGF consisted of >95% total protein, as determined by densitometric quantification of SDS-PAGE using BandScan (Glyko, Novato, CA, USA) software. The actual molecular weights of LMWP-EGF, LMWP-IGF-I, LMWP-PDGF-A, and LMWP-bFGF determined by mass spectroscopy were 8,907, 10,469, 20,642, and 19,094 Da, respectively (Figure 2A). These results matched the corresponding theoretical molecular weights. The N-terminal amino acid sequences of the LMWP-GFs were determined. These showed that LMWP had been successfully attached to the N-termini of EGF, IGF-I, PDGF-A, and bFGF and were consistent with the following theoretical sequences: Val-Ser-Arg-Arg-Arg-Arg-Arg-Arg-Gly-Gly-Arg-Arg-Arg-Arg-Asn-Ser for LMWP-EGF; Val-Ser-Arg-Arg-Arg-Arg-Arg-Arg-Gly-Gly-Arg-Arg-Arg-Arg-Gly-Pro for LMWP-IGF-I; Val-Ser-Arg-Arg-Arg-Arg-Arg-Arg-Gly-Gly-Arg-Arg-Arg-Arg-Ser-Ile for LMWP-PDGF-A; and Val-Ser-Arg-Arg-Arg-Arg-Arg-Arg-Gly-Gly-Arg-Arg-Arg-Arg-Pro-Ala for LMWP-bFGF (data not shown). The mean entrapment efficacies of LMWP-EGF, LMWP-IGF-I, LMWP-PDGF-A, and LMWP-bFGF in the Carbopol hydrogel were 92.1±2.13, 94.5±3.67, 91.8±4.10, and 95.8 ±3.92%, respectively.

To assess skin penetration by GFs after LMWP fusion, human full-thickness skin was treated with 0.1% (w/w) Carbopol hydrogel containing each individual AlexaFluor 647-labeled native or LMWP-fused GF.

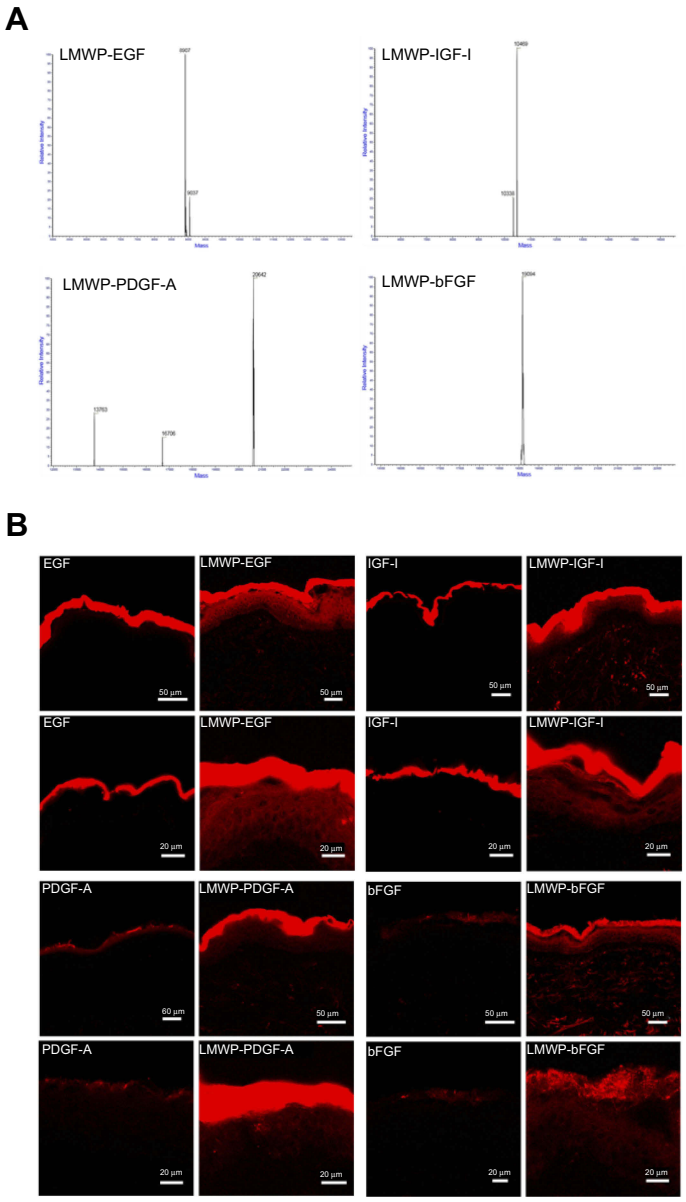

Figure 2 Characterization of LMWP-EGF, LMWP-IGF-I, LMWP-PDGF-A, and LMWP-bFGF. (**A**) Molecular weights of LMWP-EGF, LMWP-IGF-I, LMWP-PDGF-A, and LMWP-bFGF determined by liquid chromatography-electrospray ionization-tandem mass spectrometry. (**B**) Confocal laser scanning microscopy images of full-thickness human skin after 12 h treatment with 0.1% (w/w) Carbopol hydrogel containing fluorescent dye (Alexa Fluor 647) conjugated to either native GFs or LMWP-GFs: EGF and LMWP-EGF; IGF-I and LMWP-IGF-I; PDGF-A and LMWP-PDGF-A; bFGF and LMWP-bFGF.

Notes: The scale bars in the upper (20×) and lower (40×) images equal 50 and 20 μm, respectively.

Abbreviations: LMWP, low-molecular-weight protamine; GFs, growth factors; LMWP-GFs, LMWP-fused GFs; EGF, epidermal growth factor; IGF-I, insulin-like growth factor-I; PDGF-A, platelet-derived growth factor-A; bFGF, basic fibroblast growth factor; LMWP-EGF, LMWP-fused EGF; LMWP-IGF-I, LMWP-fused IGF-I; LMWP-PDGF-A, LMWP-fused PDGF-A; LMWP-bFGF, LMWP-fused bFGF.

As shown in Figure 2B, all LMWP-GFs penetrated the epidermis more effectively than did the native GFs, to become located both in the epidermis per se and the upper part of the dermis. In contrast, EGF and IGF-I were found only in the SC layer, and neither PDGF-A nor bFGF was effectively absorbed, even through the SC. Therefore, conjugation with LMWP enhanced the capacity of native GFs to penetrate skin.

Topically applied transduction domain (PTD)-conjugated peptides or proteins may enhance the treatment of skin disorders by increasing skin infiltration.[44] LMWP, which is an arginine-rich cell-penetrating peptide sequence in protamine, also showed rapid penetration through skin tissue. Studies that applied PTD and cargo complexes to animal skin have shown that short oligomers of arginine-rich intercellular delivery peptides can rapidly penetrate skin tissue.[45] The

mechanism of PTD transport through the skin has not been determined because the SC layer includes non-viable cells. The intercellular lipid domains, lipid composition, water content, and lipid/protein ratio of SC-layer cell membranes differ from those of typical cell membranes.[44,46] However, destabilization mediated by electrostatic interactions between negatively charged lipids may play a pivotal role in transporting molecules across the SC.[47] In addition, micropinocytosis, which is a rapid and lipid raft-mediated process, and actin recognition may be involved in the cellular entry and transdermal delivery of PTD-cargo complexes.[44,45,48] Furthermore, PTDs may disassemble tight junction structures within the skin, enabling them to penetrate into viable layers.[44,49,50] Finally, concentration gradients across channels or aqueous pores within the SC might enhance the infiltration of PTD-cargo complexes into different layers of the skin.[44,46] For these reasons, LMWP-GFs may have greater capacity to penetrate human skin tissue than their respective native forms.

Characterization of QCN-NE, OXY-PFOB-NE, and their hydrogel formulations

QCN was loaded into the oil phase of an o/w NE to improve its aqueous solubility and skin permeability. To obtain the optimum nanoemulsive system for QCN, various oils, surfactants, and co-surfactants were screened for solubility, and their capacity to self-emulsify and form a single-phase NE with reduced interfacial energy and no precipitation. As a result, Capryol 90 and Labrafil M1944 CS (1:1, w/w) were selected for the oil phase, Labrasol and Tween 80 (1:1, w/w) were selected as surfactants, and Cremophor EL and PEG 400 (1:1, w/w) were selected as co-surfactants to construct pseudo-ternary phase diagrams (data not shown). The surfactant and co-surfactant weight ratio for the NE (S_{mix}) was set at 3:1 (w/w), based on the capacity of the oil phase to disperse the maximum amount of hydrophobic QCN. The isotropic area for the NE at S_{mix} (3:1, w/w) was also higher than those of other NEs with S_{mix} ratios of 1:1 (w/w) and 1:3 (w/w), indicating that a higher concentration of surfactant combined with a high hydrophilic-lipophilic balance value yields high emulsification efficiency. This might be due to greater penetration of the oil phase in the hydrophobic region of the surfactant monomers, thereby reducing the interfacial tension and increasing the dispersion entropy of the oil phase in the aqueous phase.[51] Next, the optimum ratios of oil, S_{mix}, and water were determined to load the QCN, and a thermodynamically stable NE with a minimal S_{mix} concentration and high artificial skin permeability was formed (data not shown).

The optimum QCN-NE had a droplet size, PDI, and zeta potential of 19.3±0.17 nm, 0.20±0.01, and –0.34±0.13 mV, respectively. The droplet size and zeta potential of QCN-NE increased after dispersal in the hydrogel; the figures were then 71.3±1.82 nm, 0.10±0.01, and –7.63±0.924 mV, respectively. Additionally, the QCN content of QCN-NE dispersed in the hydrogel was 97.4±1.32%, indicating minimal loss of QCN during NE formation followed by dispersal in the hydrogel.

The OXY-PFOB-NE produced via microfluidization was a nanosized emulsion (average particle diameter: 227±2.39 nm; PDI: 0.18±0.03), and had a negative surface charge with a zeta potential of –2.22±0.257 mV. OXY-PFOB-NE dispersed in the hydrogel had a particle size, PDI, and zeta potential of 247±1.75 nm, 0.15±0.02, and –11.3±0.20 mV, respectively. The maximum oxygen level of OXY-PFOB-NE was approximately 23 μg/mL. This was not significantly affected by the PFOB-NE concentration, being similar to that of the PBS control, indicating that the oxygen capacity of the PFOB-NE did not change in response to hyperbaric oxygen. However, oxygen release from OXY-PFOB-NE was significantly influenced by the concentration of PFOB-NE, implying that PFOB-NE plays an important role in terms of the oxygen release rate, which can thus be controlled by the PFOB-NL concentration (Figure S1).

TEM revealed homogenous nanosized droplets of diameters <50 nm for QCN-NE and <200 nm for OXY-PFOB-NE, in agreement with the analyzer data (Figure 3A and B). In the hydrogels, QCN-NE and OXY-PFOB-NE formed irregular, nanosized globular droplets of increased (but similar) sizes, with rough surfaces, and were uniformly distributed throughout the hydrogels (Figure 3C and D). These results confirmed that the surfactants and lipids afforded thermodynamic stability to the NEs in the hydrogels by reducing the interfacial energies between immiscible liquids.

Effects of LMWP-GFs, QCN, and OXY-PFOB-NE on cell proliferation

To assess the combined biological activities of the LMWP-GFs, QCN, and oxygen, we examined the effects of LMWP-EGF, LMWP-IGF-I, LMWP-PDGF-A, LMWP-bFGF, QCN, and OXY-PFOB-NE alone or combined on the proliferation of HaCaT cells. After 24 h, combined treatment with LMWP-EGF (500 ng/mL), LMWP-IGF-I (500 ng/mL), LMWP-

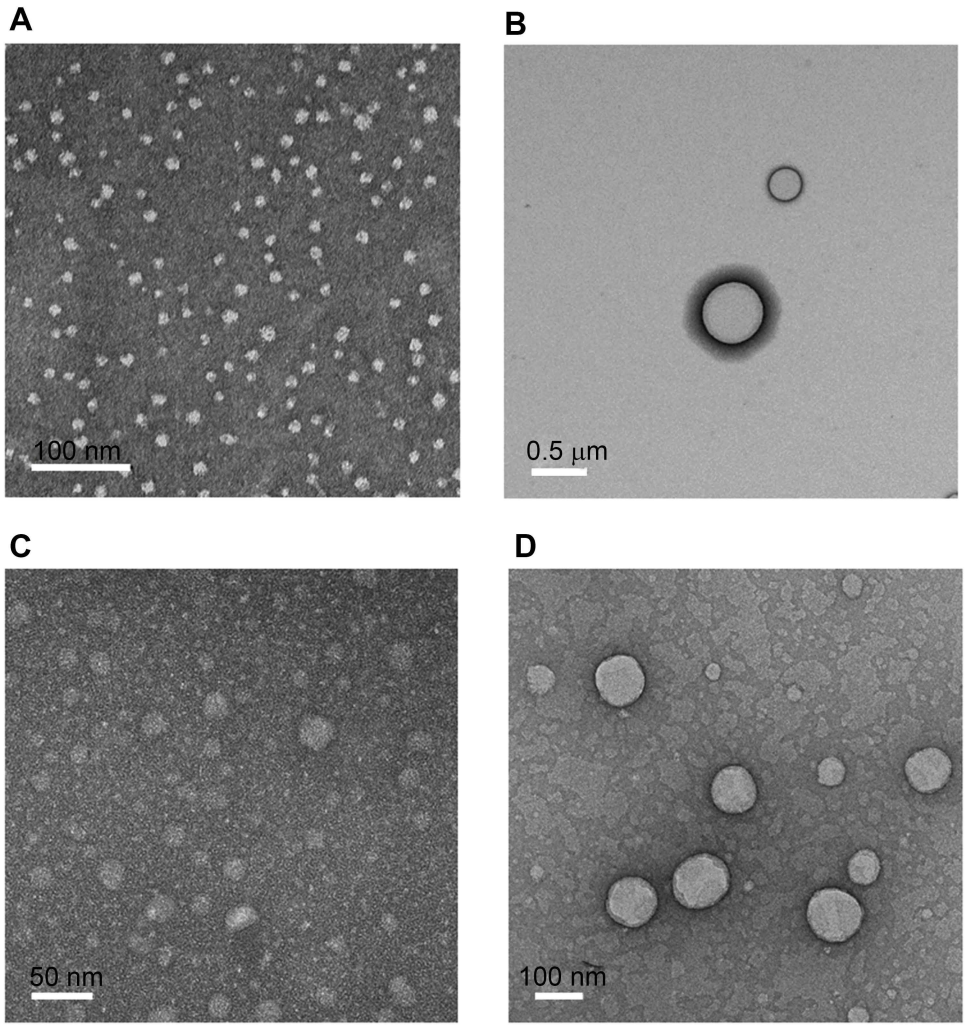

Figure 3 Characterization of QCN-NE and OXY-PFOB-NE. TEM images of (**A**) QCN-NE, (**B**) OXY-PFOB-NE, (**C**) QCN-NE dispersed in 0.1% (w/w) Carbopol hydrogel, and (**D**) OXY-PFOB-NE dispersed in 0.1% (w/w) Carbopol hydrogel.
Notes: The scale bars in (**A**), (**B**), (**C**), and (**D**) equal 100, 500, 50, and 100 nm, respectively.
Abbreviations: TEM, transmission electron microscopy; QCN, quercetin; NE, nanoemulsion; QCN-NE, QCN-loaded NE; PFOB, 1-bromoperfluorooctane; OXY-PFOB-NE, oxygen-carrying PFOB-loaded NE.

PDGF-A (10 ng/mL), and LMWP-bFGF (10 ng/mL) increased HaCaT cell proliferation by 1.34-fold compared to untreated cells, which was 16.0%, 18.4%, 27.4%, and 18.8% more cell proliferation than observed for each of these LMWP-GFs alone, respectively (Figure 4A). QCN (1 μg/mL) also increased HaCaT cell proliferation 1.17-fold compared to the control; however, this decreased as the concentration of QCN was increased to 25 μg/mL (Figure 4B). In addition, OXY-PFOB-NE activated HaCaT cell proliferation in a concentration-dependent manner, and cells treated with 30 μg/mL OXY-PFOB-NE proliferated by as much as 125% and 128% compared to untreated cells and those treated with blank PFOB-NE, respectively. However, cells cultured with 300 μg/mL OXY-PFOB-NE did not proliferate significantly, despite the high oxygen concentration (Figure 4C). Furthermore, a combined LMWP-GFs, QCN, and OXY-PFOB-NE treatment resulted in significantly more cell proliferation than treatment with each of these three components alone. Cells cultured with LMWP-GFs (LMWP-EGF [500 ng/mL], LMWP-IGF-I [500 ng/mL], LMWP-PDGF-A [10 ng/mL], and LMWP-bFGF [10 ng/mL]) and 0.1 μg/mL QCN showed 15% and 32% more proliferation than those cultured with LMWP-GFs and 0.1 μg/mL QCN, respectively. Adding 30 μg/mL OXY-PFOB-NE to a mixture of LMWP-GFs and QCN (0.1 μg/mL) increased cell proliferation by 23.2% and 11.6% compared to treatment with OXY-PFOB-NE (30 μg/mL), and a mixture of LMWP-GFs and QCN (0.1 μg/mL), respectively (Figure 4D).

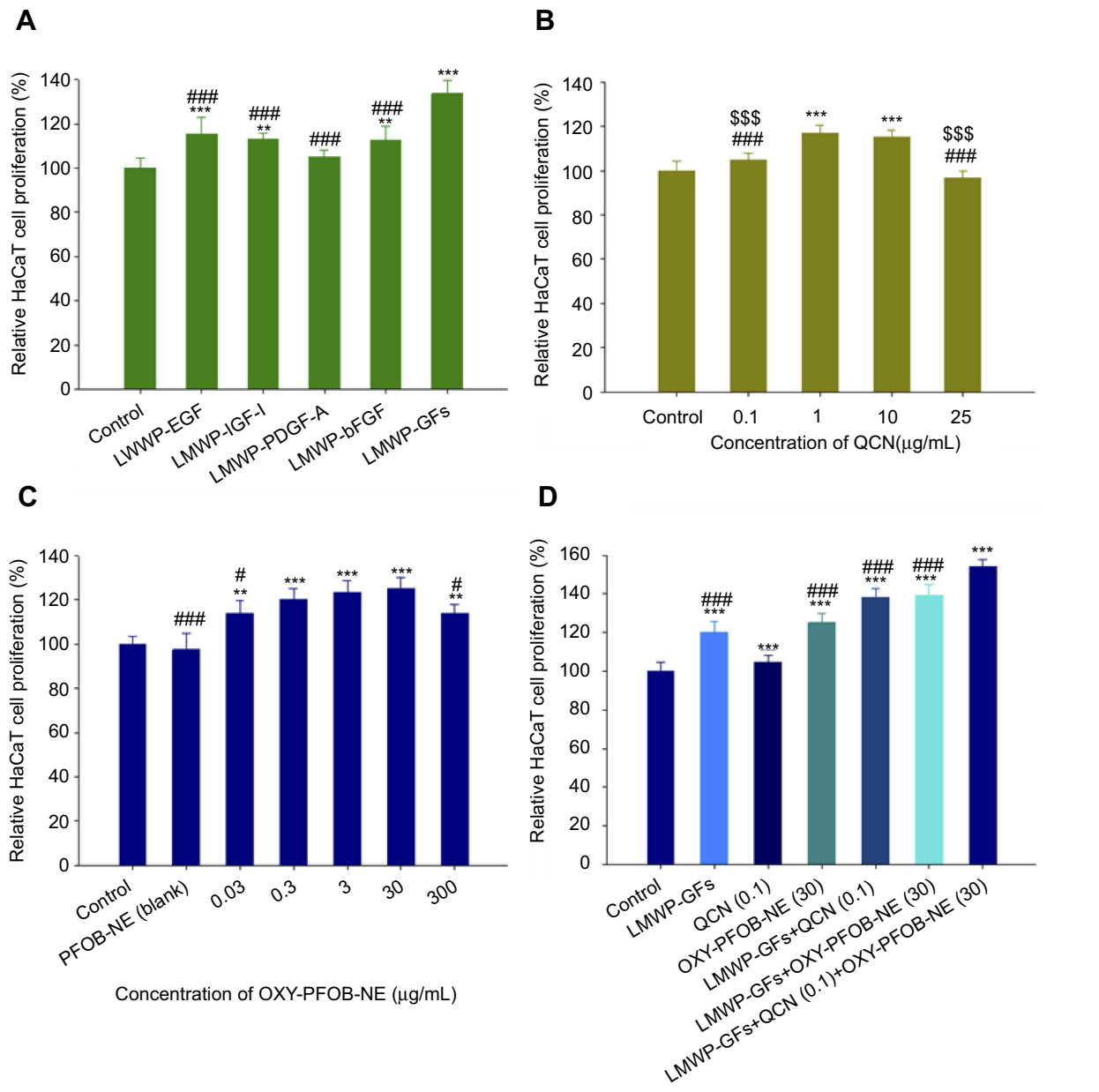

Figure 4 Keratinocyte proliferation in response to treatment with LMWP-GFs, QCN-NE, and OXY-PFOB-NE. Relative keratinocyte (HaCaT cells) proliferation after 24 h incubation with either (**A**) LMWP-GFs (***$P<0.001$ compared to the control group; ###$P<0.001$ compared to LMWP-GFs), (**B**) QCN (***$P<0.001$ compared to the control group; ###$P<0.001$ compared to QCN [1 μg/mL]; $$$$P<0.001$ compared to QCN [10 μg/mL]), (**C**) OXY-PFOB-NE (**$P<0.01$, ***$P<0.001$ compared to the control group; #$P<0.05$ compared to OXY-PFOB-NE [30 μg/mL]) alone, or (**D**) all combined. ***$P<0.001$ compared to the control group. ###$P<0.001$ compared to all LMWP-GFs, QCN, and OXY-PFOB-NE combined (LMWP-EGF [500 ng/mL] + LMWP-IGF-I [500 ng/mL] + LMWP-PDGF-A [10 ng/mL] + LMWP-bFGF [10 ng/mL] + QCN [0.1 μg/mL] + OXY-PFOB-NE [30 μg/mL]).

Notes: Cell viability was measured using WST-1 and the growth of HaCaT cells compared to the control group. All data are expressed as means ± standard deviation (n=6).

Abbreviations: LMWP, low-molecular-weight protamine; GFs, growth factors; LMWP-GFs, LMWP-fused GFs; EGF, epidermal growth factor; IGF-I, insulin-like growth factor-I; PDGF-A, platelet-derived growth factor-A; bFGF, basic fibroblast growth factor; LMWP-EGF, LMWP-fused EGF; LMWP-IGF-I, LMWP-fused IGF-I; LMWP-PDGF-A, LMWP-fused PDGF-A; LMWP-bFGF, LMWP-fused bFGF; QCN, quercetin; PFOB, 1-bromoperfluorooctane; NE, nanoemulsion; OXY-PFOB-NE, oxygen-carrying PFOB-loaded NE.

Next, we determined the effect of combining LMWP-GFs, QCN, and OXY-PFOB-NE on fibroblast cell proliferation. A combined treatment with LMWP-EGF (500 ng/mL), LMWP-IGF-I (500 ng/mL), LMWP-PDGF-A (10 ng/mL), and LMWP-bFGF (10 ng/mL) significantly increased fibroblast cell proliferation. As shown in Figure S2A, the cell proliferation value for the combined treatment was 40.1%, 18.3%, 17.5%, 15.1%, and 13.9% more than those of the control and each LMWP-GF treatment alone. When the CCD-986sk cells were treated with 0.1–25 μg/mL of QCN, the cell

proliferation value at 0.1 μg/mL QCN increased by as much as 27.3% compared to the control, but the proliferation rate reduced as the concentration of QCN was increased to 25 μg/mL (Figure S2B). Fibroblast proliferation also increased in the OXY-PFOB-NE treatment group, and the proliferation value at 30 μg/mL OXY-PFOB-NE was 34.8% and 34.0% more than that of the control and blank PFOB-NE, respectively (Figure S2C). However, these proliferation rates decreased when the concentration of OXY-PFOB-NE exceeded 30 μg/mL. Moreover, a combined treatment with LMWP-GFs, QCN (0.1 μg/mL), and OXY-PFOB-NE (30 μg/mL) significantly enhanced the proliferation of fibroblasts. This combined treatment increased cell proliferation by 20.8%, 27.2%, 32.6%, and 61.9% compared to treatment with the LMWP-GFs, QCN (0.1 μg/mL), OXY-PFOB-NE (30 μg/mL), and control, respectively (Figure S2D).

On the basis of these in vitro cell proliferation assay results, further in vitro procollagen synthesis and scratch-wound healing studies were performed using a combination of LMWP-GFs (LMWP-EGF [500 ng/mL], LMWP-IGF-I [500 ng/mL], LMWP-PDGF-A [10 ng/mL], and LMWP-bFGF [10 ng/mL]), QCN (0.1 μg/mL), and OXY-PFOB-NE (30 μg/mL).

Effects of LMWP-GFs, QCN, and OXY-PFOB-NE on procollagen synthesis

Next, the effect of combining LMWP-GFs with QCN and/or OXY-PFOB-NE on collagen synthesis by CCD-986sk cells was assessed. As shown in Figure 5, the biosynthesis of procollagen type I C-peptide was enhanced by 67.9% compared to the control group after the cells were treated with LMWP-GFs (LMWP-EGF [500 ng/mL], LMWP-IGF-I [500 ng/mL], LMWP-PDGF-A [10 ng/mL], and LMWP-bFGF [10 ng/mL]). When the cells were treated with QCN (0.1 μg/mL) or OXY-PFOB-NE (30 μg/mL), the levels of procollagen type I C-peptide were increased by 38.9% and 41.7%, respectively, compared to the control. In addition, after a combined LMWP-GFs and OXY-PFOB-NE (30 μg/mL) treatment, procollagen type I C-peptide production increased 2.01-, 1.20-, and 1.42-fold compared to treatment with the control, LMWP-GFs, and

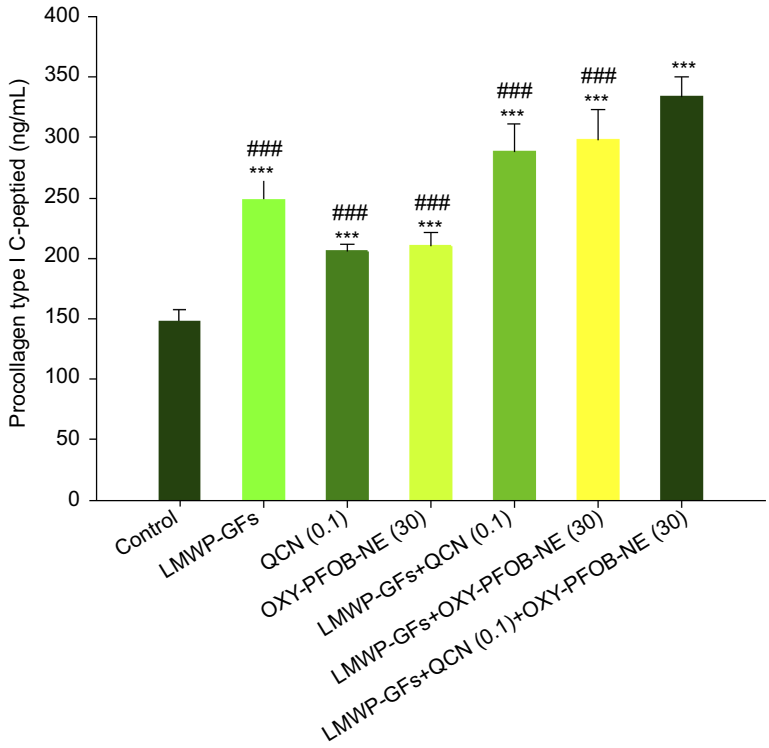

Figure 5 Collagen synthesis in response to treatment with LMWP-GFs, QCN-NE, and OXY-PFOB-NE. Synthesis of procollagen type I C-peptide in CCD-986sk cells after 24 h incubation with either LMWP-GFs, QCN, OXY-PFOB-NE alone, or all combined.

Notes: All data are expressed as means ± standard deviation (n=6). ***P<0.001 compared to the control group. ###P<0.001 compared to all LMWP-GFs, QCN, and OXY-PFOB-NE combined (LMWP-EGF [500 ng/mL] + LMWP-IGF-I [500 ng/mL] + LMWP-PDGF-A [10 ng/mL] + LMWP-bFGF [10 ng/mL] + QCN [0.1 μg/mL] + OXY-PFOB-NE [30 μg/mL]).

Abbreviations: GFs, growth factors; LMWP, low-molecular-weight protamine; LMWP-GFs, LMWP-fused GFs; EGF, epidermal growth factor; IGF-I, insulin-like growth factor-I; PDGF-A, platelet-derived growth factor-A; bFGF, basic fibroblast growth factor; LMWP-EGF, LMWP-fused EGF; LMWP-IGF-I, LMWP-fused IGF-I; LMWP-PDGF-A, LMWP-fused PDGF-A; LMWP-bFGF, LMWP-fused bFGF; QCN, quercetin; NE, nanoemulsion; QCN-NE, QCN-loaded NE; PFOB, 1-bromoperfluorooctane; OXY-PFOB-NE, oxygen-carrying PFOB-loaded NE.

OXY-PFOB-NE (30 μg/mL), respectively. The level of procollagen type I C-peptide in medium was further increased by 12.0% by adding QCN (0.1 μg/mL) to the LMWP-GFs with OXY-PFOB-NE (30 μg/mL) treatment, resulting in a 2.25-fold increase compared to the control as well as a 1.34-, 1.62-, and 1.59-fold increase compared to treatment with LMWP-GFs, QCN (0.1 μg/mL), and OXY-PFOB-NE (30 μg/mL) alone, respectively.

QCN combined with collagen may increase the hydroxyproline concentration in granulation tissue, implying enhanced production of collagen in the granulation tissue, which might be related to the antioxidant properties of QCN rather than its anti-inflammatory effect.[52] Furthermore, fibroblasts cannot synthesize collagen in the absence of molecular oxygen, which is required for the hydroxylation of proline and lysine residues in the nascent procollagen molecule.[53,54] These findings imply that collagen production by fibroblasts can be significantly enhanced by a combined treatment comprising LMWP-GFs, QCN, and OXY-PFOB-NE.

The results from the studies on the effects of cell proliferation and procollagen synthesis imply that to enhance healing, the optimum ratio for LMWP-EGF: LMWP-IGF-I:LMWP-PDGF-A:LMWP-bFGF:QCN: OXY-PFOB-NE in a hydrogel was 1:1:0.02:0.02:0.2:60.

In vitro skin permeability across a human epidermis

Improvements in the skin infiltration of EGF, IGF-I, PDGF-A, and bFGF after LMWP attachment were investigated using excised human epidermis. As shown in Figure 6A–D, the epidermal permeability of native GFs in a hydrogel was significantly improved by conjugation with LMWP. EGFs in hydrogel showed little infiltration through the human epidermis for up to 24 h; however, after a 24-h incubation, the level of infiltrated LMWP-EGF from the hydrogel was 70.2-fold higher than that of EGF, resulting in a 129-fold increase in the skin flux of LMWP-EGF. After 24 h, the cumulative LMWP-IGF-I, LMWP-PDGF-A, and LMWP-bFGF concentrations that had infiltrated across human epidermis were 2.01-, 2.98-, and 2.87-fold greater than those of each native GF, respectively. This increased the skin flux of LMWP-IGF-I (142%), LMWP-PDGF-A (161%), and LMWP-bFGF (299%) in the hydrogel compared to native GFs. The enhanced skin infiltration, which is mediated by the arginine-rich peptide LMWP, may involve macropinocytosis, actin rearrangement, and interactions between arginine and lipid phosphates in the intercellular lipid domain of the SC, leading to lipid disruption and the formation of a concentration gradient through open channels.[45,55,56] Moreover, this result indicates that an LMWP-GFs-GEL can provide efficient wound healing therapy by enhanced and sustained delivery through the lesions of more than one GF simultaneously.

The infiltration of QCN through human epidermis also significantly improved after it was incorporated into an NE and dispersed in a hydrogel (Figure 6E). QCN was detected at 6 h after loading the hydrogel containing QCN-NE, whereas QCN dispersed in 0.3% NaCMC was only observed in the receiver 24 h after loading. At 24 h, the cumulative infiltrated concentration of QCN from the QCN-NE-GEL was 1.13±0.01 μg/mL, which was 1.77-fold higher than that of QCN dispersed in 0.3% (w/v) NaCMC. Therefore, the QCN-NE-GEL displayed markedly enhanced infiltration of QCN, showing that QCN-NE may promote skin penetration by QCN. This result also demonstrated that surfactants, co-surfactants, or an oil phase play major roles in enhancing QCN infiltration through the epidermis.

When QCN is dispersed in 0.3% (w/v) NaCMC, there is no oil, surfactant, or co-surfactant. Therefore, QCN infiltration through the skin was low because the absence of these molecules limits the access and infiltration of QCN into and through the skin. Conversely, the surfactants and co-surfactants in the NE may interfere with the SC barrier, increasing the fluidity of SC lipids and facilitating drug diffusion through the barrier phase, in addition to increasing the solubility of the drug by improving the partition coefficient for QCN between the skin and the vehicle.[57–59] The mesh structure of the hydrogel matrix also hindered large droplets from diffusing into the SC.[60] Therefore, QCN-NE droplets were absorbed via a transcellular route due to their small size and the lipophilicity of the oil present. Therefore, the fact that QCN is deposited in the epidermis also demonstrates that topically applied QCN-NE-GEL has the potential for prolonged drug release around a lesion.

Oxygen transport from the OXY-PFOB-NE-GEL was also evaluated using human epidermis. Our hyperoxygenated PFOB-NE consistently increased SC oxygen tension compared to the vehicle and PBS. At 3 h after OXY-PFOB-NE-GEL treatment, the oxygen level in the receptor had reached its maximum value, which was 1.51-fold higher than that measured before loading (Figure 6F). However, the oxygen level in the receptor phase was unchanged after the non-oxygenated PFOB-NE-GEL was loaded. Overall, these data support the hypothesis that the

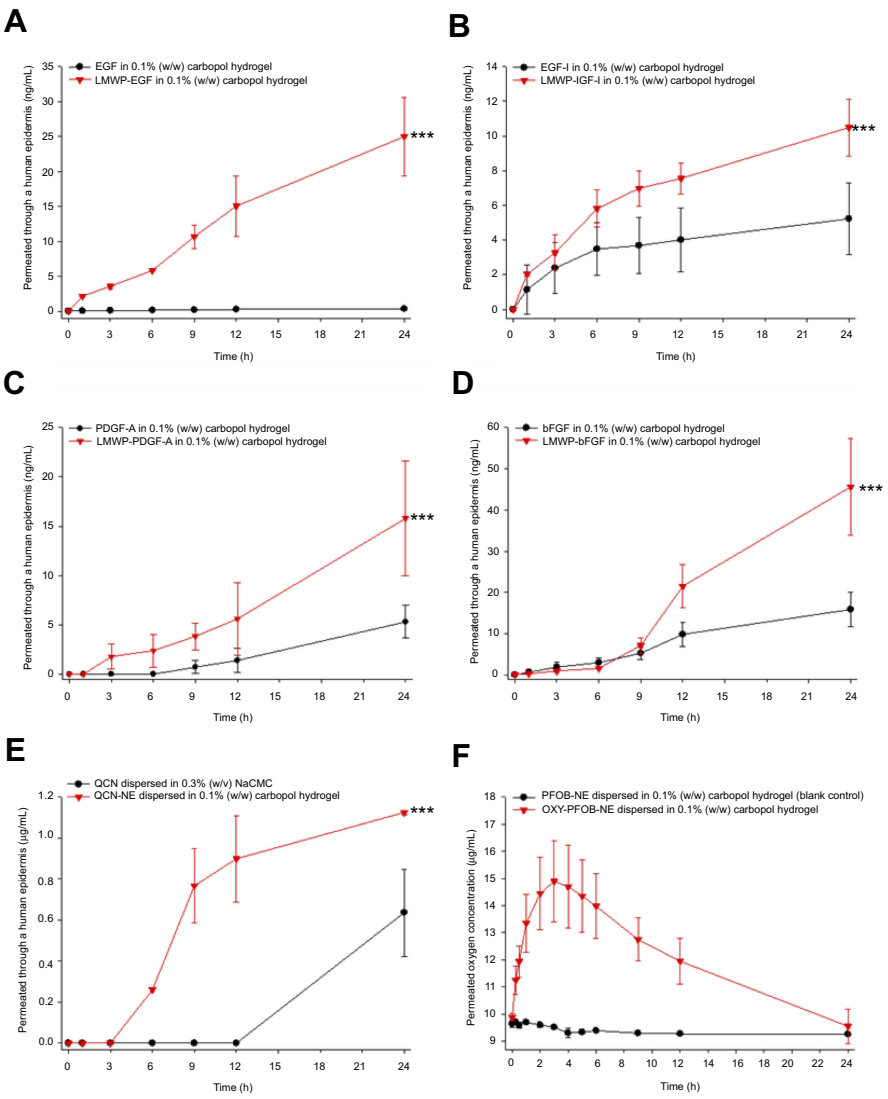

Figure 6 In vitro penetration of LMWP-GFs, QCN, and oxygen through human epidermis. Time-course showing cumulative penetration of (**A**) EGF and LMWP-EGF; (**B**) IGF-I and LMWP-IGF-I; (**C**) PDGF-A and LMWP-PDGF-A; (**D**) bFGF and LMWP-bFGF through human epidermis after incubation with each native GF or LMWP-GF in 0.1% (w/w) Carbopol hydrogel. ***P<0.001 compared to each native GF. (**E**) Time-course showing cumulative penetration of QCN through human epidermis after incubation with QCN dispersed in 0.3% (w/v) NaCMC or QCN-NE dispersed in 0.1% (w/w) Carbopol hydrogel. ***P<0.001 compared to QCN in 0.3% (w/v) NaCMC. (**F**) Time-course showing oxygen penetration though human epidermis (1 atm, 32°C) after treatment with PFOB-NE dispersed in 0.1% (w/w) Carbopol hydrogel (blank control) or OXY-PFOB-NE dispersed in 0.1% (w/w) Carbopol hydrogel.

Notes: All data are expressed as means ± standard deviation (n=6).

Abbreviations: LMWP, low-molecular-weight protamine; GFs, growth factors; LMWP-GFs, LMWP-fused GFs; EGF, epidermal growth factor; IGF-I, insulin-like growth factor-I; PDGF-A, platelet-derived growth factor-A; bFGF, basic fibroblast growth factor; LMWP-EGF, LMWP-fused EGF; LMWP-IGF-I, LMWP-fused IGF-I; LMWP-PDGF-A, LMWP-fused PDGF-A; LMWP-bFGF, LMWP-fused bFGF; QCN, quercetin; NE, nanoemulsion; QCN-NE, QCN-loaded NE; NaCMC, sodium carboxymethyl cellulose; PFOB, 1-bromoperfluorooctane; OXY-PFOB-NE, oxygen-carrying PFOB-loaded NE.

PFOB-NE-GEL can sequester and deliver oxygen via PFOB-NE, thereby supplying oxygen locally through the epidermis to the wound for 24 h.

Effects of a hydrogel containing LMWP-GFs, QCN-NE, and OXY-PFOB-NE on in vitro scratch-wound recovery

To evaluate the effects of LMWP-GFs, QCN, and oxygen on keratinocyte and fibroblast proliferation/migration, in vitro wound recovery assays were performed in the presence of hydrogels containing LMWP-GFs, QCN-NE, and OXY-PFOB-NE, alone or combined. As expected, the LMWP-GFs treatment led to rapid scratch-wound closure in keratinocytes. At 10 h after treatment, the recovery rate of wounds treated with the LMWP-GFs-GEL containing LMWP-EGF (500 ng/mL), LMWP-IGF-I (500 ng/mL), LMWP-PDGF-A (10 ng/mL), and LMWP-bFGF (10 ng/mL) was 74.6% higher than that of wounds in the untreated control group. In addition, at

10 h after treatment, both the QCN-NE-GEL and OXY-PFOB-NE-GEL accelerated wound closure in keratinocytes by 26.0% and 60.6% compared to the control group, respectively (Figure 7A). When the keratinocytes were treated with the hydrogel comprising LMWP-GFs and QCN-NE, they had improved wound closure rates at 10 h of 94.8%, 11.6%, 54.5%, and 21.3% compared to the control, LMWP-GFs-GEL, QCN-NE-GEL, and OXY-PFOB-NE-GEL treatments, respectively. We also looked for synergistic effects on wound closure after treatment with a hydrogel containing LMWP-GFs, QCN-NE, and OXY-PFOB-NE and found that wound recovery rates at 10 h were accelerated by as much as 96.7%, 12.7%, 56.1%, and 22.5% compared to the control, LMWP-GFs-GEL, QCN-NE-GEL, and OXY-PFOB-NE-GEL, respectively. This corresponded to a wound recovery rate of 98.0±2.91% at 12 h after treatment (Figure 7B). On the other hand, wound recovery rates of 54.0±5.52%, 92.1±4.42%, 68.9±3.53%, and 94.5±1.41% were observed in the control, LMWP-GFs-GEL, QCN-NE-GEL, and OXY-PFOB-NE-GEL groups at 12 h after treatment, respectively (Figure 7C).

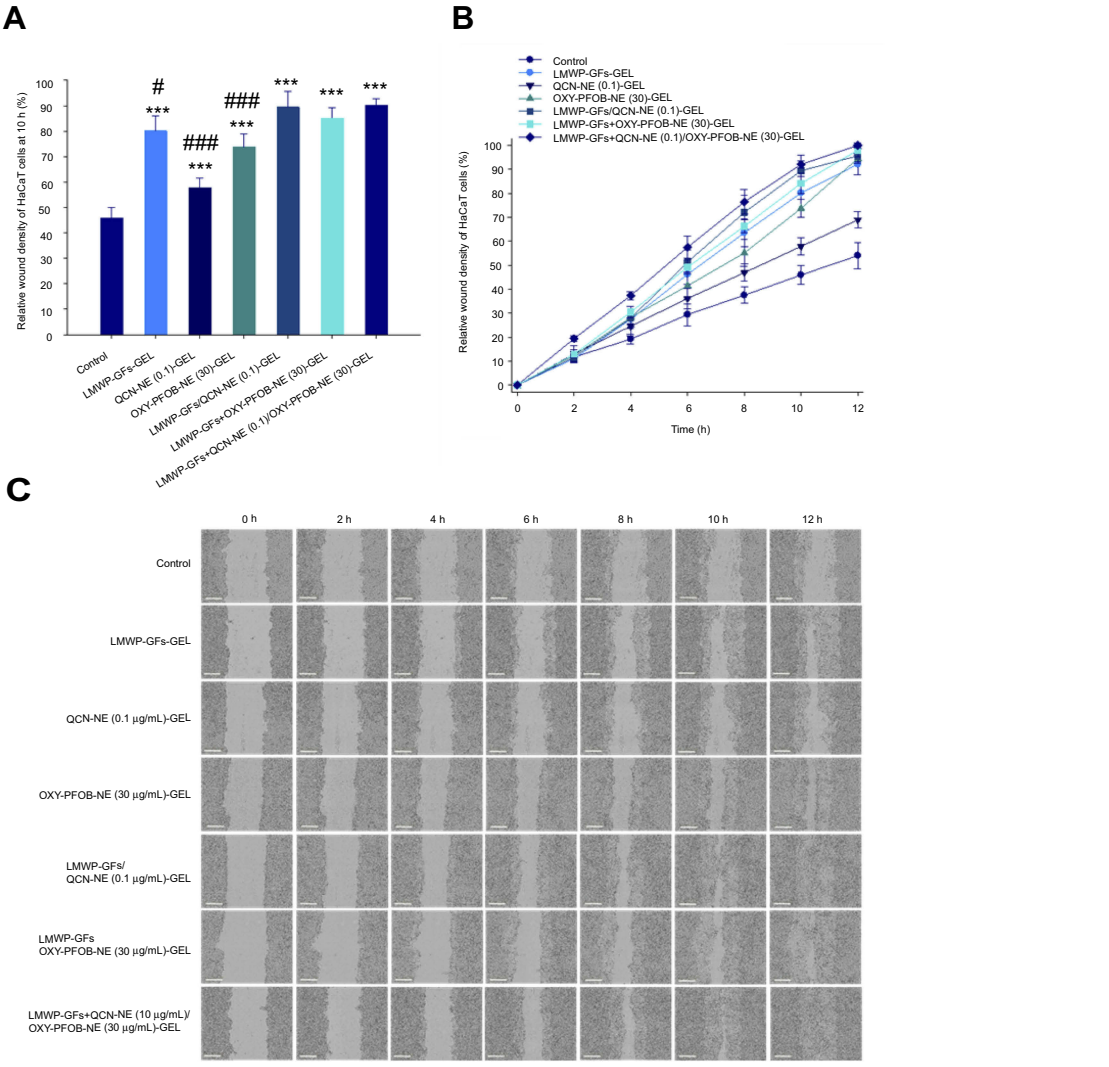

Figure 7 In vitro scratch-wound healing in keratinocytes following treatment with LMWP-GFs, QCN-NE, and OXY-PFOB-NE. (**A**) Relative scratch-wound recovery of HaCaT cells at 10 h. (**B**) Time-course showing relative scratch-wound recovery. (**C**) Representative microscopic images of HaCaT cell scratch-wounds at 0, 2, 4, 6, 8, 10, and 12 h after incubation with serum-free medium (control) or Carbopol hydrogel containing either LMWP-GFs, QCN-NE, OXY-PFOB-NE alone, or all combined.

Notes: All data are expressed as means ± standard deviation (n=6). ***P<0.001 compared to the control group. #P<0.05, ###P<0.001 compared to all LMWP-GFs, QCN-NE, and OXY-PFOB-NE combined (LMWP-EGF [500 ng/mL] + LMWP-IGF-I [500 ng/mL] + LMWP-PDGF-A [10 ng/mL] + LMWP-bFGF [10 ng/mL] + QCN-NE [0.1 μg/mL QCN] + OXY-PFOB-NE [30 μg/mL]). The scale bar in (C) equals 300 μm.

Abbreviations: LMWP, low-molecular-weight protamine; GFs, growth factors; LMWP-GFs, LMWP-fused GFs; EGF, epidermal growth factor; IGF-I, insulin-like growth factor-I; PDGF-A, platelet-derived growth factor-A; bFGF, basic fibroblast growth factor; LMWP-EGF, LMWP-fused EGF; LMWP-IGF-I, LMWP-fused IGF-I; LMWP-PDGF-A, LMWP-fused PDGF-A; LMWP-bFGF, LMWP-fused bFGF; QCN, quercetin; NE, nanoemulsion; QCN-NE, QCN-loaded NE; PFOB, 1-bromoperfluorooctane; OXY-PFOB-NE, oxygen-carrying PFOB-loaded NE.

In the fibroblast cells, a combined treatment with LMWP-GFs, QCN-NE, and OXY-PFOB-NE also led to significantly enhanced scratch-wound closure compared to cells treated with each component alone. The recovery rates at 24 h after treatment with LMWP-GFs-GEL, QCN-NE-GEL (0.1 μg/mL QCN), or OXY-PFOB-NE-GEL (30 μg/mL PFOB-NE) were 76.6%, 61.8%, and 42.7% greater than those of the control group, respectively (Figure S3A). In comparison, a synergistic effect on wound closure was observed after a combined treatment with LMWP-GFs, QCN-NE, and OXY-PFOB-NE, which accelerated wound closure in fibroblast cells by as much as 110% compared to the control. Wound closure for the combined treatment was 1.19-, 1.30-, and 1.49-fold greater than that in cells cultured with LMWP-GFs-GEL, QCN-NE-GEL, or OXY-PFOB-NE-GEL alone, respectively. In addition, combined treatment with LMWP-GFs, QCN-NE (0.1 μg/mL QCN), and OXY-PFOB-NE (30 μg/mL PFOB-NE) resulted in 13% and 19% greater wound recovery rates than those found after treatment with a hydrogel containing LMWP-GFs and QCN-NE, or a LMWP-GFs and QCN-NE-loaded hydrogel, respectively. At 36 h after treatment, complete wound closure was observed in cells treated with LMWP-GFs/QCN-NE/OXY-PFOB-NE-GEL (97.1±4.58% of wound closed) (Figure S3B). In contrast, cell-free zones remained in the control group and in fibroblasts treated with LMWP-GFs-GEL, QCN-NE-GEL, or OXY-PFOB-NE-GEL alone (wound recovery: control, 60.8±4.87%; LMWP-GFs-GEL, 89.2±3.33%; QCN-NE-GEL, 81.8±3.64%; and OXY-PFOB-NE, 86.9±5.17%; Figure S3C).

Effects of a hydrogel containing LMWP-GFs, QCN-NE, and OXY-PFOB-NE on the diabetic mouse wound model

Next, we investigated the effects of LMWP-GFs, QCN-NE, and an OXY-PFOB-NE-loaded hydrogel on the healing of full-thickness wounds in diabetic mice. As shown in Figure 8, natural wound-healing in diabetic mice was significantly delayed (approximately 70% recovery after 12 days) compared to that of non-diabetic mice. No mouse became infected during treatment. After treatment with LMWP-GFs-GEL, the diabetic wounds were significantly reduced compared to those treated with the hydrogel alone (diabetic control), and to those treated with QCN-NE-GEL or OXY-PFOB-NE-GEL. Additionally, diabetic wounds treated with LMWP-GFs-GEL tended to close more rapidly from day 3 compared to the QCN-NE-GEL and OXY-PFOB-NE-GEL groups. Therefore, at 6 days after treatment, the diabetic mice treated with LMWP-GFs-GEL showed 29.6%, 16.1%, and 17.0% greater reductions in wound area than diabetic control, QCN-NE-GEL, and OXY-PFOB-NE-GEL groups, respectively (Figure 8A).

A treatment that combines several GFs may promote chronic wound repair. The most promising combination of GFs to enhance the mitogenic response of diabetic ulcer fibroblasts may include PDGF with IGF-I, bFGF, or EGF.[26,27,61] Therefore, in this study, LMWP-fused EGF, IGF-I, PDGF-A, and bFGF in a concentration ratio of 50:50:1:1 were used to accelerate re-epithelialization and connective tissue formation, from the early stages of healing.[26,27] IGF-I can reportedly act synergistically with EGF to promote the migration and proliferation of keratinocytes by upregulating the EGF receptor, resulting in an increase in the synthesis of fibronectin and other connective tissue molecules and stimulation of cell proliferation.[62] Therefore, as the epithelial cells advance to form the first layer that covers the wound, keratinocytes proliferate to ensure that there are enough cells, and LMWP-EGF combined with LMWP-IGF-I may play an important role in the proliferative process. PDGF is a potent activator of collagen synthesis and acts as a mitogen in fibroblasts, increasing the cell density in the loosely arranged sub-epithelial connective tissue.[18] However, the organization and maturation of the collagen fibers, and epithelialization were enhanced more significantly by a combined treatment with PDGF with IGF-I, which might be due to the progression of fibroblasts into the S phase of the cell cycle and the production of EGF in the proliferating fibroblasts.[63] Furthermore, addition of PDGF and bFGF simultaneously led to a significantly greater response in diabetic ulcer fibroblasts than their sequential addition, implying that the presence of more than one GF may be required for diabetic ulcer fibroblasts to maximize DNA synthesis.[64] This might be due to the limited number of receptors, low GF-receptor binding affinity, dysfunctional intracellular signal transduction, or increased expression of inhibitory substrates such as IGF-I BP-3.[65] Therefore, in this study, keratinocytes and fibroblasts provided with a combination of LMWP-GFs exhibited significantly enhanced cell proliferation/migration in vitro, and diabetic wounds treated with LMWP-GFs-GEL showed accelerated re-epithelialization and connective tissue formation in the early stages of wound healing compared to those treated with the blank hydrogel in vivo.

In addition, the wounds treated with QCN-NE-GEL or OXY-PFOB-NE-GEL alone also closed more rapidly than those of the diabetic control. However, these diabetic wound healing effects were observed from 6 days after treatment. The wound recovery rates in the QCN-NE-GEL

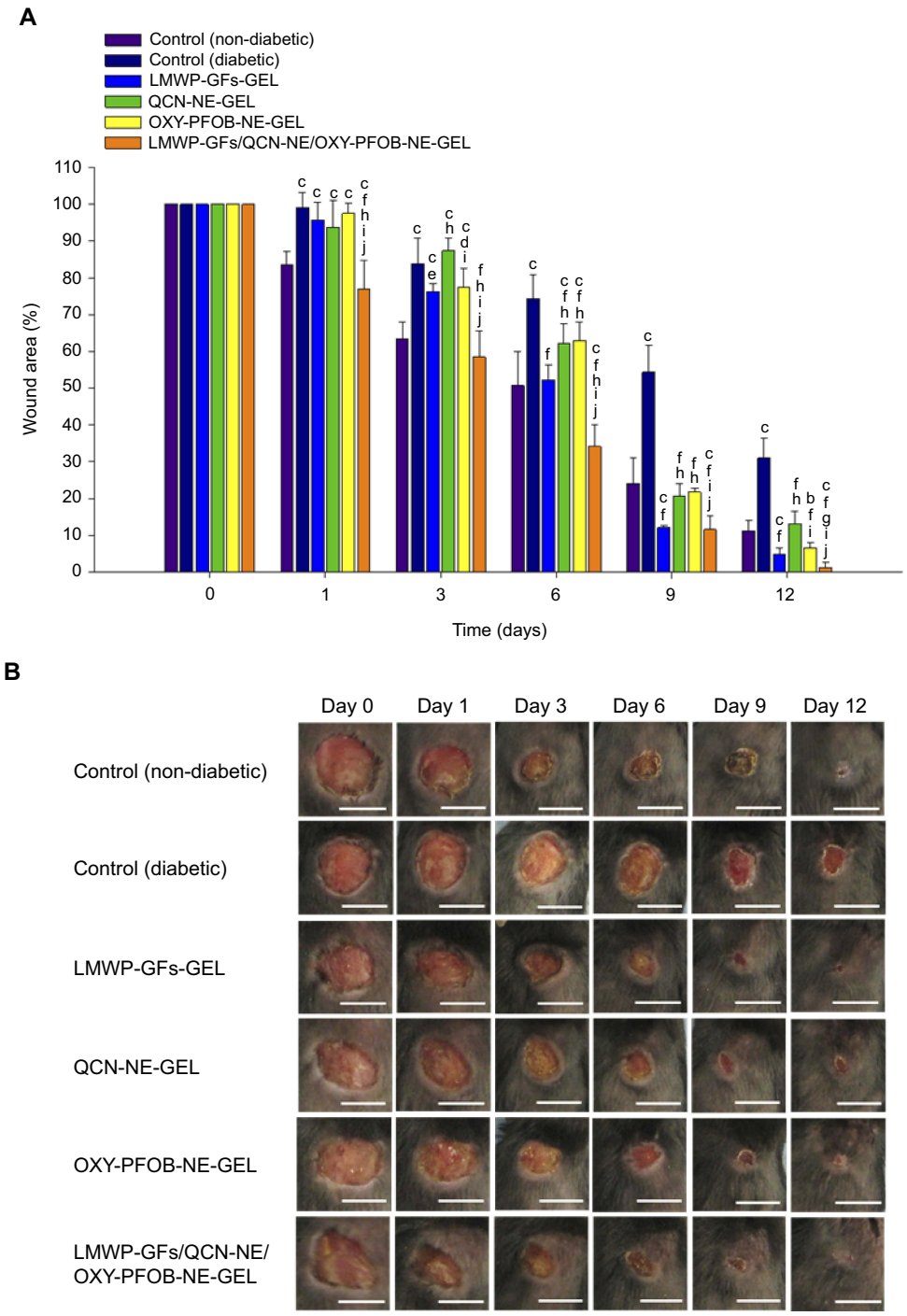

Figure 8 In vivo diabetic wound closure following treatment with hydrogels containing LMWP-GFs, QCN-NE, and OXY-PFOB-NE. Progression of wound closure in a full-thickness excisional diabetic mouse wound model following treatment with Carbopol hydrogel containing either LMWP-GFs, QCN-NE, OXY-PFOB-NE alone, or all combined. (**A**) The wound area was measured over 12 days. (**B**) Representative photographs of non-diabetic and diabetic wounds treated with vehicle (0.1% [w/w] Carbopol hydrogel), and diabetic wounds treated with LMWP-GFs-GEL (0.1% [w/w] Carbopol hydrogel containing LMWP-EGF [100 μg/mL], LMWP-IGF-I [100 μg/mL], LMWP-PDGF-A [2 μg/mL], and LMWP-bFGF [2 μg/mL]), QCN-NE-GEL (0.1% [w/w] Carbopol hydrogel containing QCN-NE [20 μg/mL QCN]), PFOB-NE-GEL (0.1% [w/w] Carbopol hydrogel containing oxygen-carrying PFOB-NE [6 mg/mL]), and LMWP-GFs/QCN-NE/OXY-PFOB-NE-GEL (0.1% [w/w] Carbopol hydrogel containing LMWP-EGF [100 μg/mL], LMWP-IGF-I [100 μg/mL], LMWP-PDGF-A [2 μg/mL], LMWP-bFGF [2 μg/mL], QCN-NE [20 μg/mL QCN], and OXY-PFOB-NE [6 mg/mL PFOB-NE]).

Notes: All data are expressed as means ± standard deviation (n=15). [a]$P<0.05$, [b]$P<0.01$, [c]$P<0.001$ compared to the control (non-diabetic). [d]$P<0.05$, [e]$P<0.01$, [f]$P<0.001$ compared to the control (diabetic). [g]$P<0.05$, [h]$P<0.001$ compared to the LMWP-GFs-GEL. [i]$P<0.001$ compared to the QCN-NE-GEL. [j]$P<0.001$ compared to the PFOB-NE-GEL. The scale bar in (B) equals 10 mm.

Abbreviations: LMWP, low-molecular-weight protamine; GFs, growth factors; LMWP-GFs, LMWP-fused GFs; EGF, epidermal growth factor; IGF-I, insulin-like growth factor-I; PDGF-A, platelet-derived growth factor-A; bFGF, basic fibroblast growth factor; LMWP-EGF, LMWP-fused EGF; LMWP-IGF-I, LMWP-fused IGF-I; LMWP-PDGF-A, LMWP-fused PDGF-A; LMWP-bFGF, LMWP-fused bFGF; QCN, quercetin; NE, nanoemulsion; QCN-NE, QCN-loaded NE; PFOB, 1-bromoperfluorooctane; OXY-PFOB-NE, oxygen-carrying PFOB-loaded NE.

and OXY-PFOB-NE-GEL groups were 62% and 60% higher than those in the diabetic control group at 9 days after treatment, respectively (Figure 8A).

These results also confirmed that sufficient QCN and oxygen had been absorbed from the hydrogels through the wounded skin, enhancing fibroblast proliferation and metabolism. QCN may suppress uncontrolled inflammation, and block histamine release and the expression of pro-inflammatory cytokines in mast cells, preventing acute skin inflammation.[32] QCN also increases collagen production and cross-linking, as well as protecting tissues and proteins from oxidative damage because it acts as a lipid peroxidation and MMP activation inhibitor.[66] Furthermore, oxygen availability can have a profound influence on repair processes. During the early stages of wound healing, reduced nicotinamide adenine dinucleotide (NADH) oxidase produces superoxide radicals in the presence of oxygen, which help to prevent bacterial infections.[67] Oxygen also regulates angiogenesis and can enhance cell motility and proliferation. Several studies have shown that wound oxygenation is closely related to the rate of wound healing via accelerating collagen synthesis and improved proline hydroxylase enzyme activity.[68] This may be because oxygen is necessary for the synthesis of hydroxyproline, which is one of the building blocks of collagen.[67] The resulting fibrillogenesis increases the tensile strength of collagen and improves wound remodeling in the proliferative phase of healing.[69,70] Therefore, these results imply that oxygen from OXY-PFOB-NE accelerated regeneration compared to the diabetic control.

Overall, the main targets for QCN-NE-GEL and OXY-PFOB-NE-GEL in the wound healing process are fibroblasts and the formation of granulation tissue. The granulation layer is the first to form from the base of the wound. This highly vascularized new connective tissue catalyzes skin regeneration by restoring the vascular network, which provides nutrients, oxygen and access to the new tissues, cells, and progenitors. It also provides a matrix for keratinocytes to migrate along, activating re-epithelialization from the wound edges. Re-epithelialization is critical for restoring barrier function in successful chronic wound healing.[71] Therefore, in this study, the delay in initial wound reduction after treatment with QCN-NE-GEL or OXY-PFOB-NE-GEL may be due to delayed proliferation/migration of epithelial cells.

In contrast, diabetic wound healing was significantly accelerated from day 1 to 12 after the mice were treated with LMWP-GFs/QCN-NE/OXY-PFOB-NE-GEL. Treatment with LMWP-GFs/QCN-NE/OXY-PFOB-NE-GEL induced a significant reduction in the wound area, especially in the first 3 days after treatment. The wound-healing rate for the LMWP-GFs/QCN-NE/OXY-PFOB-NE-GEL treatment group was 30.3%, 23.3%, 33.0%, and 24.5% faster than those of the diabetic control, LMWP-GFs-GEL, QCN-NE-GEL, and OXY-PFOB-NE-GEL groups, respectively (Figure 8A). Six days after treatment, the LMWP-GFs/QCN-NE/OXY-PFOB-NE-GEL diabetic wound healing efficacy was still superior to all other treatment groups, including the non-diabetic control group, and the wound recovery was 156%, 37.9%, 74.4%, and 77.6% greater than those of the diabetic control, LMWP-GFs-GEL, QCN-NE-GEL, and OXY-PFOB-NE-GEL groups, respectively (Figure 8A). The remaining wound sizes at day 9 were: 11.6±3.65% for the LMWP-GFs/QCN-NE/OXY-PFOB-NE-GEL group, 12.1±0.623% for the LMWP-GFs-GEL group, 20.7±3.33% for the QCN-NE-GEL group, and 21.8±1.09% for the OXY-PFOB-NE-GEL group (Figure 8A). At day 12, all wounds treated with LMWP-GFs/QCN-NE/OXY-PFOB-NE-GEL appeared to be completely closed (1.25±1.35%), whereas 31.0±5.44%, 4.76±1.71%, 13.2±3.45%, and 6.56±1.53% of the wounds still remained in the diabetic control, LMWP-GFs-GEL, QCN-NE-GEL, and OXY-PFOB-NE-GEL groups, respectively (Figure 8B). These results indicate synergistic interactions among the bioactivity of LMWP-GFs and the intrinsic healing properties of QCN and oxygen. Enhanced delivery to and increased concentrations of LMWP-GFs, QCN, and oxygen in the wound bed may also be important, because this guarantees sustained and controlled levels of these critical components at the wound site during the healing process.

Histological analysis of the wound site

Next, to confirm the enhanced wound healing efficacy of the hydrogel comprising LMWP-GFs, QCN-NE, and OXY-PFOB-NE in the diabetic mice, new tissue formation in the wound area was analyzed histologically at different time points after treatment by staining with H&E, CK6, α-SMA, and MT (Figure 9). Compared to the non-diabetic mice, re-epithelization of the wounds in the diabetic control mice was significantly delayed (Figure 9A). Specifically, in the non-diabetic mice, the wounds were rapidly covered with a fibrin clot and then re-epithelialization occurred from the lower to upper part of the wound, with basal cells in the epidermis covering the scar.[72] Re-epithelialization in the diabetic wounds occurred over the granulation and inflammatory tissue as the repair process progressed, regardless of

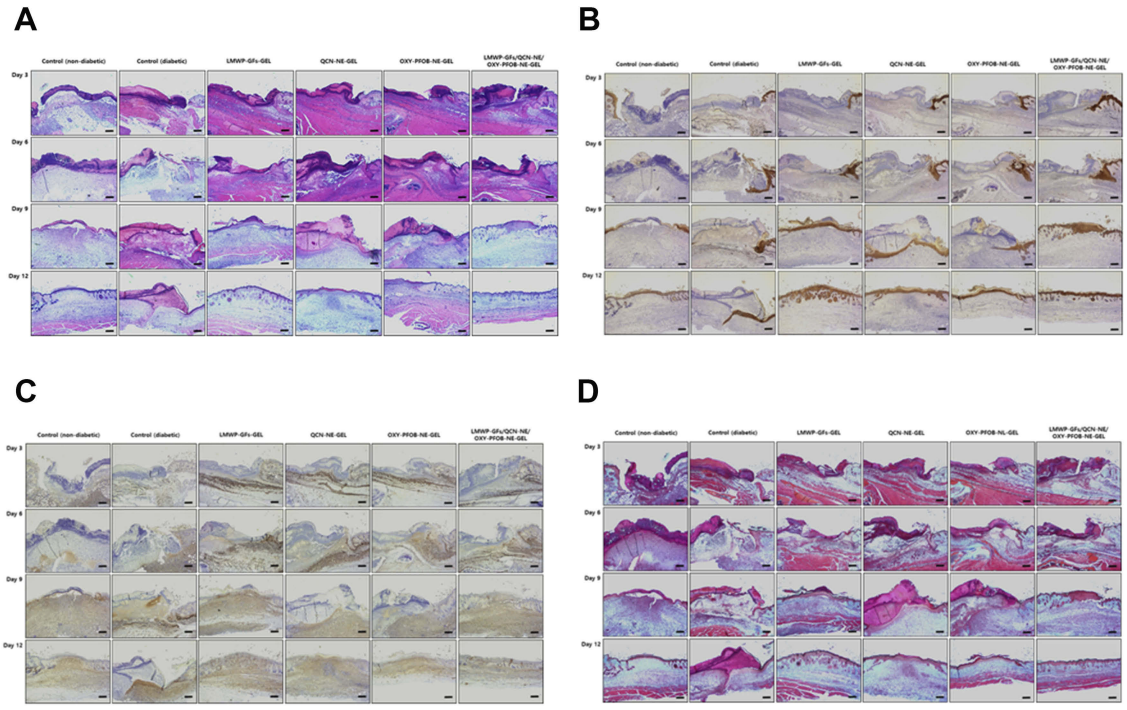

Figure 9 Histological analysis during wound closure. The Carbopol hydrogel containing LMWP-GFs, QCN-NE, and OXY-PFOB-NE enhanced re-epithelialization and granulation tissue-formation in full-thickness skin wounds of diabetic mice within 12 days. Representative light micrograph images of sections from the wounds stained with (**A**) H&E to assess re-epithelialization, (**B**) CK6 (brown) as a marker for activated keratinocytes around the wound edge, (**C**) α-SMA (brown) to identify differentiated myofibroblasts in the wound, and (**D**) MT (blue) to identify collagen fibers in the wound at 3, 6, 9, and 12 days after treatment.

Notes: The scale bar equals 50 μm.

Abbreviations: LMWP, low-molecular-weight protamine; GFs, growth factors; LMWP-GFs, LMWP-fused GFs; QCN, quercetin; NE, nanoemulsion; QCN-NE, QCN-loaded NE; PFOB, 1-bromoperfluorooctane; OXY-PFOB-NE, oxygen-carrying PFOB-loaded NE; H&E, hematoxylin & eosin; CK6, cytokeratin 6; α-SMA, α-smooth muscle actin; MT; Masson's trichrome.

treatment type (Figure 9A). Therefore, on day 3, all the treatments stimulated epidermal layer formation, and more fibroblasts and inflammatory cells were recruited from the wound margin to the wound site compared to the diabetic control (Figure 9A).

After 3 days of treatment with LMWP-GFs/QCN-NE/OXY-PFOB-NE-GEL, the diabetic wounds were completely covered with a thick scab and the newly formed epidermal layer around the wound edge had migrated further into the wound bed than in the other treatment groups. This observation correlated with the CK6 (brown color) immunostaining, which indicated significant activation of keratinocytes in the basal compartment near the wound edge (Figure 9B). Immunohistological staining with α-SMA (brown color) was used to explore the transformation of fibroblasts into myofibroblasts, which are responsible for the contraction of granulation tissue during tissue repair. More myofibroblasts had infiltrated the wounds treated with LMWP-GFs, QCN-NE, or PFOB-NE-GEL alone compared to those treated with LMWP-GFs/QCN-NE/OXY-PFOB-NE-GEL (Figure 9C). This is probably because the initial wound contraction, which is regulated by contractile myofibroblasts, occurs more rapidly (within 3 days) after treatment with LMWP-GFs/QCN-NE/OXY-PFOB-NE-GEL.[73] Wound contraction is an important process in wound healing, especially for chronic wounds such as DFUs, but excessive contraction may lead to scar formation.[74,75] In addition, the production of a collagen matrix was more pronounced in diabetic skin, particularly after LMWP-GFs/QCN-NE/OXY-PFOB-NE-GEL treatment, than it was in other treatment groups (Figure 9D).

On day 6, the diabetic wounds treated with LMWP-GFs-GEL or LMWP-GFs/QCN-NE/OXY-PFOB-NE-GEL showed greater CK6 immunostaining around the wound edge, indicating enhanced epidermal regeneration with larger thicker re-epithelialized areas than in the other groups (Figure 9A and B). In addition, loosely packed collagen fibers and granulation tissue with irregular arrangements were also observed in the LMWP-GFs-GEL, OXY-PFOB-NE-GEL, and LMWP-GFs/QCN-NE/OXY-PFOB-NE-GEL treatment groups (Figure 9C and D). These results indicate

that high expression of myofibroblasts within 6 days can stimulate contraction of the wound and have beneficial effects in the early stages of healing. This may imply that in diabetic mice treated with LMWP-GFs/QCN-NE/OXY-PFOB-NE-GEL, granulation tissue fills the wound bed in the early phase of wound healing, potentiated by the proliferation of skin fibroblasts. Treatment with QCN-NE-GEL also led to rapid wound healing, but a larger fibrin clot developed over the diabetic wound. This may be due to wound contraction induced by fibroblast migration and the production of a collagen matrix.

After 9 days, wounds treated with the LMWP-GFs-GEL had a complete epithelium overlaying the scar and reduced inflammation. This was supported by the loose conjunctive tissue that had been present from the onset of healing. Different levels of collagen deposition were observed among the diabetic control mice (Figures 9A and B). Inflammation persisted in the wound beds of the diabetic mice but the surface of the wounds treated with QCN-NE-GEL had a complete epithelium overlaying the scar. The granulation tissue in the diabetic wounds remained in the dermis at 9 days after wounding, with overgrowing fibroblast proliferation. However, the scar produced after QCN-NE-GEL treatment was more pronounced than that produced after the LMWP-GFs-GEL treatment. Although treatment with the OXY-PFOB-NE-GEL also produced a remarkable amount of new tissue infiltration and scaffold degranulation, the wounds showed incomplete epidermal re-epithelialization and a large scar until 9 days after treatment (Figures 9C and D). In contrast, a fibrin clot significantly decreased in size and a complete epithelial layer formed on the upper surface of the diabetic wound site in the LMWP-GFs/QCN-NE/OXY-PFOB-NE-GEL group. Moreover, the lesion was completely replaced by new tissue, accompanied by obvious collagen deposition at the periphery. Therefore, the collagen alignment was more regular in the LMWP-GFs/QCN-NE/OXY-PFOB-NE-GEL group than in the LMWP-GFs-GEL, QCN-NE-GEL, and OXY-PFOB-NE-GEL groups. At this time point, fibroblasts play an important role in collagen synthesis and scar formation.[76] During the re-epithelialization phase, the initial ECM is gradually replaced by a collagen matrix and new blood vessels form.[71,72] Therefore, the LMWP-GFs/QCN-NE/OXY-PFOB-NE-GEL was superior to all other treatments in terms of the total collagen produced in the maturing granulation bed.

After 12 days of treatment, wound tissue fibrosis was still incomplete and a fibrin clot was more marked in the diabetic control group (Figure 9A and B). In addition, cell migration and inflammation were visible beyond the proliferating cells at the wound margin. A loosely packed collagen matrix was observed in the diabetic control (Figure 9C and D). The wound site treated with the LMWP-GFs/QCN-NE/OXY-PFOB-NE-GEL had a well-organized epithelium and multiple cell layers with significant keratinization (Figure 9A and B). Furthermore, in the LMWP-GFs/QCN-NE/OXY-PFOB-NE-GEL group, dermal papillae and skin appendages, such as hair follicles and sebaceous glands, were fully developed in contrast to wounds treated with QCN-NE-GEL or OXY-PFOB-NE-GEL (Figure 9A and B). Unlike the wounds treated with LMWP-GFs-GEL and QCN-NE-GEL, wounds treated with LMWP-GFs/QCN-NE/OXY-PFOB-NE-GEL showed thin granulation tissue with more densely packed mature collagen fibers arranged in parallel and well-organized reticular dermal layers (Figure 9C and D). Some infiltrating inflammatory cells remained at wound sites in the QCN-NE-GEL and OXY-PFOB-NE-GEL groups, indicating a transition from the proliferative phase of tissue regeneration to tissue remodeling (Figure 9A and D). In contrast to wounds treated with LMWP-GFs/QCN-NE/OXY-PFOB-NE-GEL, loosely packed irregular collagen fibers were still observed in the wounds treated with LMWP-GFs-GEL or QCN-NE (Figure 9C and D).

As previously reported, a combination of LMWP-appended GFs stimulated wound healing with rapid and extensive re-epithelialization and dermal tissue remodeling in a diabetic mouse model.[27] In this study, QCN-NE-GEL or OXY-PFOB-NE-GEL also enhanced healing by increasing fibroblast proliferation, but little effect on keratinocyte proliferation has been observed in vivo, implying that proliferative activity may be specific to fibroblasts. A combined treatment of LMWP-GFs with QCN-NE and OXY-PFOB-NE significantly reduced the wound area, especially in the first 3 days after wounding, in diabetic mice. This was probably due to stimulation of wound contraction, which has a beneficial effect in the early stages of healing. In diabetic mice treated with LMWP-GFs/QCN-NE/OXY-PFOB-NE-GEL, granulation tissue fills the wound bed in the early phase of healing. This is potentiated by the proliferation of fibroblasts and results in a faster healing profile in diabetic wounds than in all the other treatment groups. The highest fibroblast density and the production of a collagen matrix were most evident in diabetic skin, particularly after treatment with the LMWP-GFs/QCN-NE/OXY-PFOB-NE-GEL.

Taken together, these results imply that synergistic interactions occur among the intrinsic healing properties of LMWP-GFs and the biological activities of QCN-NE and OXY-PFOB-NE. These interactions enhance fibroblast proliferation and collagen production, promoting healing by targeting several cell types in a timely manner during the complex wound repair process. Nevertheless, further studies are needed to optimize treatment concentrations in vivo and define the biological mechanisms responsible for the synergistic interactions that are important in diabetic wound repair. Using these optimal treatment concentrations would stimulate the regeneration and repair of non-healing ulcers and other types of chronic and acute wounds.

Conclusion

This study demonstrated that a topical Carbopol hydrogel system comprising LMWP-GFs, QCN-NE, and OXY-PFOB-NE significantly enhanced diabetic wound recovery due to increased and prolonged skin infiltration of the LMWP-GFs, QCN, and oxygen from OXY-PFOB-NE, and synergistic healing activities. The LMWP-GFs, QCN-NE, and OXY-PFOB-NE combination had synergistic effects on the proliferation of keratinocytes and fibroblasts, and on procollagen synthesis by fibroblasts. The optimal proportions of LMWP-EGF, LMWP-IGF-I, LMWP-PDGF-A, LMWP-bFGF, QCN-NE, and OXY-PFOB-NE were 1, 1, 0.02, 0.02, 0.2, and 60, respectively. Moreover, the Carbopol hydrogel containing LMWP-GFs, QCN-NE, and OXY-PFOB-NE significantly improved scratch-wound recovery in keratinocytes and fibroblasts in vitro compared to hydrogels consisting of each component alone. Therefore, the LMWP-GFs/QCN-NE/OXY-PFOB-NE-GEL significantly accelerated wound healing in the diabetic mouse model, showing prolonged positive effects that decreased wound size by as much as 54%, 35%, 45%, and 46% compared to vehicle, LMWP-GFs-GEL, QCN-NE-GEL, and OXY-PFOB-NE-GEL treatment, respectively. In addition, improved re-epithelialization, thicker and more mature granulation tissue, and more extensive collagen deposition were observed in mice treated with LMWP-GFs/QCN-NE/OXY-PFOB-NE-GEL compared to the other treatments. These results imply LMWP-GFs/QCN-NE/OXY-PFOB-NE-GEL may be used for clinical management of chronic wounds, including DFUs.

Acknowledgments

This research was supported by the Basic Research Program through the National Research Foundation of Korea (NRF), funded by the Ministry of Education (NRF-2017R1D1A1B03032283).

Disclosure

The authors report no conflicts of interest in this work.

References

1. Singer AJ, Clark RA. Cutaneous wound healing. *N Engl J Med*. 1999;341(10):738–746. doi:10.1056/NEJM199909023411006
2. Fonder MA, Lazarus GS, Cowan DA, Aronson-Cook B, Kohli AR, Mamelak AJ. Treating the chronic wound: A practical approach to the care of nonhealing wounds and wound care dressings. *J Am Acad Dermatol*. 2008;58(2):185–206. doi:10.1016/j.jaad.2007.08.048
3. Frykberg RG, Banks J. Challenges in the treatment of chronic wounds. *Adv Wound Care*. 2015;4(9):560–582. doi:10.1089/wound.2015.0635
4. Lipsky BA, Berendt AR, Cornia PB, et al. Infectious Diseases Society of America clinical practice guideline for the diagnosis and treatment of diabetic foot infections. *Clin Infect Dis*. 2012;54(12):e132–173.
5. Boulton AJM, Armstrong DG, Albert SF, et al. Comprehensive foot examination and risk assessment. *Diabetes Care*. 2008;31(8):1679–1685. doi:10.2337/dc07-1868
6. Yager DR, Chen SM, Ward SI, Olutoye OO, Diegelmann RF, Kelman Cohen I. Ability of chronic wound fluids to degrade peptide growth factors is associated with increased levels of elastase activity and diminished levels of proteinase inhibitors. *Wound Repair Regen*. 1997;5(1):23–32. doi:10.1046/j.1524-475X.1997.50108.x
7. Cook H, Davies KJ, Harding KG, Thomas DW. Defective extracellular matrix reorganization by chronic wound fibroblasts is associated with alterations in TIMP-1, TIMP-2, and MMP-2 activity. *J Invest Dermatol*. 2000;115(2):225–233. doi:10.1046/j.1523-1747.2000.00044.x
8. Baynes JW. Role of oxidative stress in development of complications in diabetes. *Diabetes*. 1991;40(4):405–412. doi:10.2337/diab.40.4.405
9. Gao S, Tang G, Hua D, et al. Stimuli-responsive bio-based polymeric systems and their applications. *J Mater Chem B*. 2019;7(5):709–729.
10. Duan G, Greiner A. Air-blowing-assisted coaxial electrospinning toward high productivity of core/sheath and hollow fibers. *Macromol Mater Eng*. 2019;304(5):1–5. doi:10.1002/mame.v304.5
11. Jiang S, Han D, Huang C, Duan G, Hou H. Temperature-induced molecular orientation and mechanical properties of single electrospun polyimide nanofiber. *Mater Lett*. 2018;216:81–83. doi:10.1016/j.matlet.2017.12.146
12. Lv D, Wang R, Tang G, et al. Ecofriendly electrospun membranes loaded with visible-light-responding nanoparticles for multifunctional usages: highly efficient air filtration, dye scavenging, and bactericidal activity. *ACS Appl Mater Interfaces*. 2019;11(13):12880–12889. doi:10.1021/acsami.9b01508
13. Brem H, Tomic-Canic M. Cellular and molecular basis of wound healing in diabetes. *J Clin Invest*. 2007;117(5):1219–1222. doi:10.1172/JCI32169
14. Barrientos S, Stojadinovic O, Golinko MS, Brem H, Tomic-Canic M. Growth factors and cytokines in wound healing. *Wound Repair Regen*. 2008;16(5):585–601. doi:10.1111/j.1524-475X.2008.00410.x
15. Lee K, Silva EA, Mooney DJ. Growth factor delivery-based tissue engineering: general approaches and a review of recent developments. *J R Soc Interface*. 2011;8(55):153–170. doi:10.1098/rsif.2010.0223

16. Pierce GF, Mustoe TA. Pharmacologic enhancement of wound healing. *Annu Rev Med*. 1995;46:467–481. doi:10.1146/annurev.med.46.1.467
17. Marti-Carvajal AJ, Gluud C, Nicola S, et al. Growth factors for treating diabetic foot ulcers. *Cochrane Database Syst Rev*. 2015. doi:10.1002/14651858.CD008548.pub2
18. Lynch SE, Colvin RB, Antoniades HN. Growth factors in wound healing. Single and synergistic effects on partial thickness porcine skin wounds. *J Clin Invest*. 1989;84(2):640–646. doi:10.1172/JCI114210
19. Jazwa A, Kucharzewska P, Leja J, et al. Combined vascular endothelial growth factor-A and fibroblast growth factor 4 gene transfer improves wound healing in diabetic mice. *Genet Vaccines Ther*. 2010;8:1–6. doi:10.1186/1479-0556-8-6
20. Schultz GS, Sibbald RG, Falanga V, et al. Wound bed preparation: a systematic approach to wound management. *Wound Repair Regen*. 2003;11(Suppl 1):S1–S28. doi:10.1046/j.1524-475X.11.s2.1.x
21. Jain R, Agarwal A, Kierski PR, et al. The use of native chemical functional groups presented by wound beds for the covalent attachment of polymeric microcarriers of bioactive factors. *Biomaterials*. 2013;34(2):340–352. doi:10.1016/j.biomaterials.2012.09.055
22. Losi P, Briganti E, Errico C, et al. Fibrin-based scaffold incorporating VEGF- and bFGF-loaded nanoparticles stimulates wound healing in diabetic mice. *Acta Biomater*. 2013;9(8):7814–7821. doi:10.1016/j.actbio.2012.10.038
23. Yoo Y, Hyun H, Yoon S-J, et al. Visible light-cured glycol chitosan hydrogel dressing containing endothelial growth factor and basic fibroblast growth factor accelerates wound healing in vivo. *J Ind Eng Chem*. 2018;67:365–372. doi:10.1016/j.jiec.2018.07.009
24. Li X, Ye X, Qi J, et al. EGF and curcumin co-encapsulated nanoparticle/hydrogel system as potent skin regeneration agent. *Int J Nanomed*. 2016;11:3993–4009. doi:10.2147/IJN.S104350
25. Zhang X, Kang X, Jin L, Bai J, Liu W, Wang Z. Stimulation of wound healing using bioinspired hydrogels with basic fibroblast growth factor (bFGF). *Int J Nanomed*. 2018;13:3897–3906. doi:10.2147/IJN.S168998
26. Bae IH, Park JW, Kim DY. Enhanced regenerative healing efficacy of a highly skin-permeable growth factor nanocomplex in a full-thickness excisional mouse wound model. *Int J Nanomed*. 2014;9:4551–4567.
27. Choi JU, Lee SW, Pangeni R, Byun Y, Yoon IS, Park JW. Preparation and in vivo evaluation of cationic elastic liposomes comprising highly skin-permeable growth factors combined with hyaluronic acid for enhanced diabetic wound-healing therapy. *Acta Biomater*. 2017;57:197–215. doi:10.1016/j.actbio.2017.04.034
28. Decharneux T, Dubois F, Beauloye C, Wattiaux-De Coninck S, Wattiaux R. Effect of various flavonoids on lysosomes subjected to an oxidative or an osmotic stress. *Biochem Pharmacol*. 1992;44(7):1243–1248. doi:10.1016/0006-2952(92)90521-J
29. Martin A. The use of antioxidants in healing. *Dermatol Surg*. 1996;22(2):156–160. doi:10.1111/j.1524-4725.1996.tb00499.x
30. Skaper SD, Fabris M, Ferrari V, Dalle Carbonare M, Leon A. Quercetin protects cutaneous tissue-associated cell types including sensory neurons from oxidative stress induced by glutathione depletion: cooperative effects of ascorbic acid. *Free Radic Biol Med*. 1997;22(4):669–678. doi:10.1016/S0891-5849(96)00383-8
31. Vedakumari WS, Ayaz N, Karthick AS, Senthil R, Sastry TP. Quercetin impregnated chitosan-fibrin composite scaffolds as potential wound dressing materials - Fabrication, characterization and in vivo analysis. *Eur J Pharm Sci*. 2017;97:106–112. doi:10.1016/j.ejps.2016.11.012
32. Hatahet T, Morille M, Hommoss A, Devoisselle JM, Muller RH, Begu S. Quercetin topical application, from conventional dosage forms to nanodosage forms. *Eur J Pharm Biopharm*. 2016;108:41–53. doi:10.1016/j.ejpb.2016.08.011
33. Rothwell JA, Day AJ, Morgan MR. Experimental determination of octanol-water partition coefficients of quercetin and related flavonoids. *J Agric Food Chem*. 2005;53(11):4355–4360. doi:10.1021/jf0483669
34. Sen CK. Wound healing essentials: let there be oxygen. *Wound Repair Regen*. 2009;17(1):1–18. doi:10.1111/j.1524-475X.2008.00436.x
35. Kalani M, Brismar K, Fagrell B, Ostergren J, Jorneskog G. Transcutaneous oxygen tension and toe blood pressure as predictors for outcome of diabetic foot ulcers. *Diabetes Care*. 1999;22(1):147–151. doi:10.2337/diacare.22.1.147
36. Prato M, Magnetto C, Jose J, et al. 2H,3H-decafluoropentane-based nanodroplets: new perspectives for oxygen delivery to hypoxic cutaneous tissues. *PLoS One*. 2015;10(3):1–20. doi:10.1371/journal.pone.0119769
37. Niinikoski J, Hunt TK, Dunphy JE. Oxygen supply in healing tissue. *Am J Surg*. 1972;123(3):247–252. doi:10.1016/0002-9610(72)90277-2
38. Bernatchez SF, Tucker J, Chiffoleau G. Hyperbaric oxygen therapy and oxygen compatibility of skin and wound care products. *Adv Wound Care*. 2017;6(11):371–381. doi:10.1089/wound.2017.0742
39. Davis SC, Cazzaniga AL, Ricotti C, et al. Topical oxygen emulsion: a novel wound therapy. *Arch Dermatol*. 2007;143(10):1252–1256. doi:10.1001/archderm.143.10.1252
40. Wijekoon A, Fountas-Davis N, Leipzig ND. Fluorinated methacrylamide chitosan hydrogel systems as adaptable oxygen carriers for wound healing. *Acta Biomater*. 2013;9(3):5653–5664.
41. Choi JK, Jang JH, Jang WH, et al. The effect of epidermal growth factor (EGF) conjugated with low-molecular-weight protamine (LMWP) on wound healing of the skin. *Biomaterials*. 2012;33(33):8579–8590. doi:10.1016/j.biomaterials.2012.07.061
42. Choi SW, Pangeni R, Jung DH, Kim SJ, Park JW. Construction and characterization of cell-penetrating peptide-fused fibroblast growth factor and vascular endothelial growth factor for an enhanced percutaneous delivery system. *J Nanosci Nanotechnol*. 2018;18(2):842–847. doi:10.1166/jnn.2018.14864
43. Pangeni R, Kang S-W, Oak M, Park EY, Park JW. Oral delivery of quercetin in oil-in-water nanoemulsion: in vitro characterization and in vivo anti-obesity efficacy in mice. *J Funct Foods*. 2017;38:571–581. doi:10.1016/j.jff.2017.09.059
44. Nasrollahi SA, Taghibiglou C, Azizi E, Farboud ES. Cell-penetrating peptides as a novel transdermal drug delivery system. *Chem Biol Drug Des*. 2012;80(5):639–646. doi:10.1111/cbdd.12008
45. Hou YW, Chan MH, Hsu HR, et al. Transdermal delivery of proteins mediated by non-covalently associated arginine-rich intracellular delivery peptides. *Exp Dermatol*. 2007;16(12):999–1006. doi:10.1111/j.1600-0625.2007.00622.x
46. Rothbard JB, Garlington S, Lin Q, et al. Conjugation of arginine oligomers to cyclosporin A facilitates topical delivery and inhibition of inflammation. *Nat Med*. 2000;6:1253–1257. doi:10.1038/81359
47. Desai P, Patlolla RR, Singh M. Interaction of nanoparticles and cell-penetrating peptides with skin for transdermal drug delivery. *Mol Membr Biol*. 2010;27(7):247–259. doi:10.3109/09687680903507080
48. Lopes LB, Furnish E, Komalavilas P, et al. Enhanced skin penetration of P20 phosphopeptide using protein transduction domains. *Eur J Pharm Biopharm*. 2008;68(2):441–445. doi:10.1016/j.ejpb.2007.05.001
49. Ohtake K, Maeno T, Ueda H, Natsume H, Morimoto Y. Poly-L-arginine predominantly increases the paracellular permeability of hydrophilic macromolecules across rabbit nasal epithelium in vitro. *Pharm Res*. 2003;20(2):153–160. doi:10.1023/A:1022485816755
50. Morita K, Miyachi Y. Tight junctions in the skin. *J Dermatol Sci*. 2003;31(2):81–89.
51. Soliman KA, Ibrahim HK, Ghorab MM. Formulation of avanafil in a solid self-nanoemulsifying drug delivery system for enhanced oral delivery. *Eur J Pharm Sci*. 2016;93:447–455. doi:10.1016/j.ejps.2016.08.050
52. Gomathi K, Gopinath D, Rafiuddin Ahmed M, Jayakumar R. Quercetin incorporated collagen matrices for dermal wound healing processes in rat. *Biomaterials*. 2003;24(16):2767–2772. doi:10.1016/S0142-9612(03)00059-0
53. Hackam DJ, Ford HR. Cellular, biochemical, and clinical aspects of wound healing. *Surg Infect (Larchmt)*. 2002;3(Suppl 1):S23–S35. doi:10.1089/sur.2002.3.s1-23

54. Togami K, Miyao A, Miyakoshi K, Kanehira Y, Tada H, Chono S. Efficient delivery to human lung fibroblasts (WI-38) of pirfenidone incorporated into liposomes modified with truncated basic fibroblast growth factor and its inhibitory effect on collagen synthesis in idiopathic pulmonary fibrosis. *Biol Pharm Bull*. 2015;38(2):270–276. doi:10.1248/bpb.b14-00659
55. Futaki S. Membrane-permeable arginine-rich peptides and the translocation mechanisms. *Adv Drug Deliv Rev*. 2005;57(4):547–558. doi:10.1016/j.addr.2004.10.009
56. Kaplan IM, Wadia JS, Dowdy SF. Cationic TAT peptide transduction domain enters cells by macropinocytosis. *J Control Release*. 2005;102(1):247–253. doi:10.1016/j.jconrel.2004.10.018
57. Kreilgaard M. Influence of microemulsions on cutaneous drug delivery. *Adv Drug Deliv Rev*. 2002;54:S77–S98. doi:10.1016/S0169-409X(02)00116-3
58. Vicentini FT, Simi TR, Del Ciampo JO, et al. Quercetin in w/o microemulsion: in vitro and in vivo skin penetration and efficacy against UVB-induced skin damages evaluated in vivo. *Eur J Pharm Biopharm*. 2008;69(3):948–957. doi:10.1016/j.ejpb.2008.01.012
59. Rai VK, Mishra N, Yadav KS, Yadav NP. Nanoemulsion as pharmaceutical carrier for dermal and transdermal drug delivery: formulation development, stability issues, basic considerations and applications. *J Control Release*. 2018;270:203–225. doi:10.1016/j.jconrel.2017.11.049
60. Zheng Y, Ouyang WQ, Wei YP, et al. Effects of Carbopol((R)) 934 proportion on nanoemulsion gel for topical and transdermal drug delivery: a skin permeation study. *Int J Nanomed*. 2016;11:5971–5987. doi:10.2147/IJN.S119286
61. Obara K, Ishihara M, Ishizuka T, et al. Photocrosslinkable chitosan hydrogel containing fibroblast growth factor-2 stimulates wound healing in healing-impaired db/db mice. *Biomaterials*. 2003;24(20):3437–3444. doi:10.1016/S0142-9612(03)00220-5
62. Krane JF, Murphy DP, Carter DM, Krueger JG. Synergistic effects of epidermal growth factor (EGF) and insulin-like growth factor I/somatomedin C (IGF-I) on keratinocyte proliferation may be mediated by IGF-I transmodulation of the EGF receptor. *J Invest Dermatol*. 1991;96(4):419–424. doi:10.1111/1523-1747.ep12469799
63. Lynch SE, Nixon JC, Colvin RB, Antoniades HN. Role of platelet-derived growth factor in wound healing: synergistic effects with other growth factors. *Proc Natl Acad Sci U S A*. 1987;84(21):7696–7700. doi:10.1073/pnas.84.21.7696
64. Loot MA, Kenter SB, Au FL, et al. Fibroblasts derived from chronic diabetic ulcers differ in their response to stimulation with EGF, IGF-I, bFGF and PDGF-AB compared to controls. *Eur J Cell Biol*. 2002;81(3):153–160. doi:10.1078/0171-9335-00228
65. Giannini S, Mohan S, Kasuya J, et al. Characterization of insulin-like growth factor-binding proteins produced by cultured fibroblasts from patients with noninsulin-dependent diabetes mellitus, insulin-dependent diabetes mellitus, or obesity. *J Clin Endocrinol Metab*. 1994;79(6):1824–1830.
66. Cho JW, Cho SY, Lee SR, Lee KS. Onion extract and quercetin induce matrix metalloproteinase-1 in vitro and in vivo. *Int J Mol Med*. 2010;25(3):347–352.
67. Patil PS, Fountas-Davis N, Huang H, et al. Fluorinated methacrylamide chitosan hydrogels enhance collagen synthesis in wound healing through increased oxygen availability. *Acta Biomater*. 2016;36:164–174. doi:10.1016/j.actbio.2016.03.022
68. Gordillo GM, Sen CK. Evidence-based recommendations for the use of topical oxygen therapy in the treatment of lower extremity wounds. *Int J Low Extrem Wounds*. 2009;8(2):105–111. doi:10.1177/1534734609335149
69. Harrison BS, Eberli D, Lee SJ, Atala A, Yoo JJ. Oxygen producing biomaterials for tissue regeneration. *Biomaterials*. 2007;28(31):4628–4634. doi:10.1016/j.biomaterials.2007.07.003
70. Phang JM, Liu W, Hancock CN, Fischer JW. Proline metabolism and cancer: emerging links to glutamine and collagen. *Curr Opin Clin Nutr Metab Care*. 2015;18(1):71–77. doi:10.1097/MCO.0000000000000121
71. Evans ND, Oreffo RO, Healy E, Thurner PJ, Man YH. Epithelial mechanobiology, skin wound healing, and the stem cell niche. *J Mech Behav Biomed Mater*. 2013;28:397–409. doi:10.1016/j.jmbbm.2013.04.023
72. Moura LI, Dias AM, Leal EC, Carvalho L, de Sousa HC, Carvalho E. Chitosan-based dressings loaded with neurotensin–an efficient strategy to improve early diabetic wound healing. *Acta Biomater*. 2014;10(2):843–857. doi:10.1016/j.actbio.2013.09.040
73. Moulin V, Auger FA, Garrel D, Germain L. Role of wound healing myofibroblasts on re-epithelialization of human skin. *Burns*. 2000;26(1):3–12. doi:10.1016/S0305-4179(99)00091-1
74. Ono I, Tateshita T, Inoue M. Effects of a collagen matrix containing basic fibroblast growth factor on wound contraction. *J Biomed Mater Res*. 1999;48(5):621–630. doi:10.1002/(ISSN)1097-4636
75. Ishihara M, Ono K, Sato M, et al. Acceleration of wound contraction and healing with a photocrosslinkable chitosan hydrogel. *Wound Repair Regen*. 2001;9(6):513–521. doi:10.1046/j.1524-475x.2001.00513.x
76. Devalliere J, Dooley K, Hu Y, Kelangi SS, Uygun BE, Yarmush ML. Co-delivery of a growth factor and a tissue-protective molecule using elastin biopolymers accelerates wound healing in diabetic mice. *Biomaterials*. 2017;141:149–160. doi:10.1016/j.biomaterials.2017.06.043

Supplementary materials

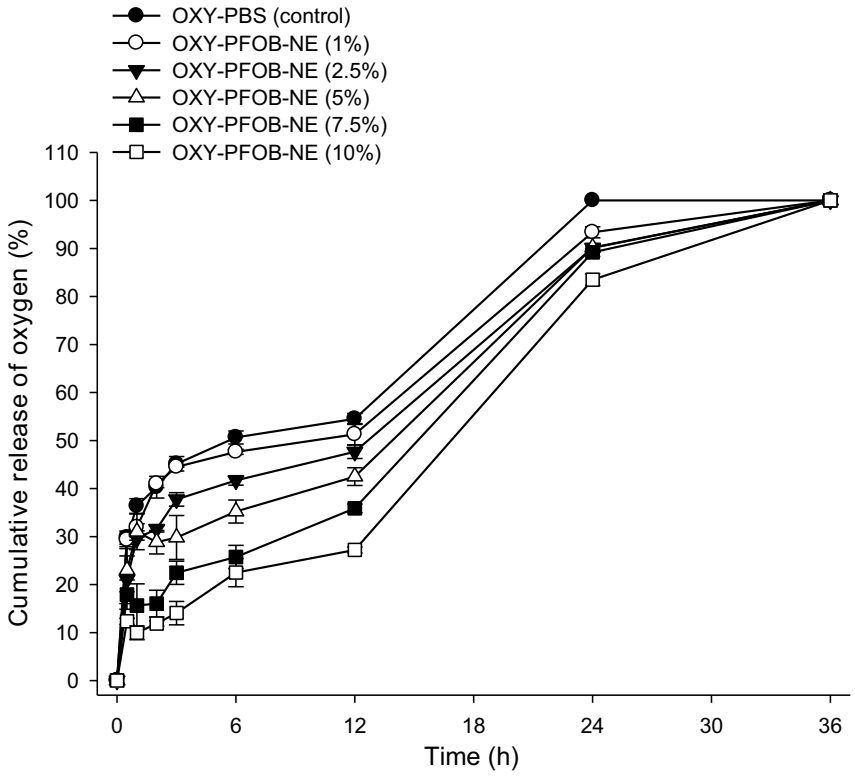

Figure S1 Cumulative oxygen release from OXY-PFOB-NE at different PFOB-NE concentrations in 5% CO_2 (air) under static conditions at 37°C.
Notes: All data are expressed as mean ± standard deviation (n=6).
Abbreviations: PFOB, 1-bromoperfluorooctane; NE, nanoemulsion; OXY-PFOB-NE, oxygen-carrying PFOB-loaded NE.

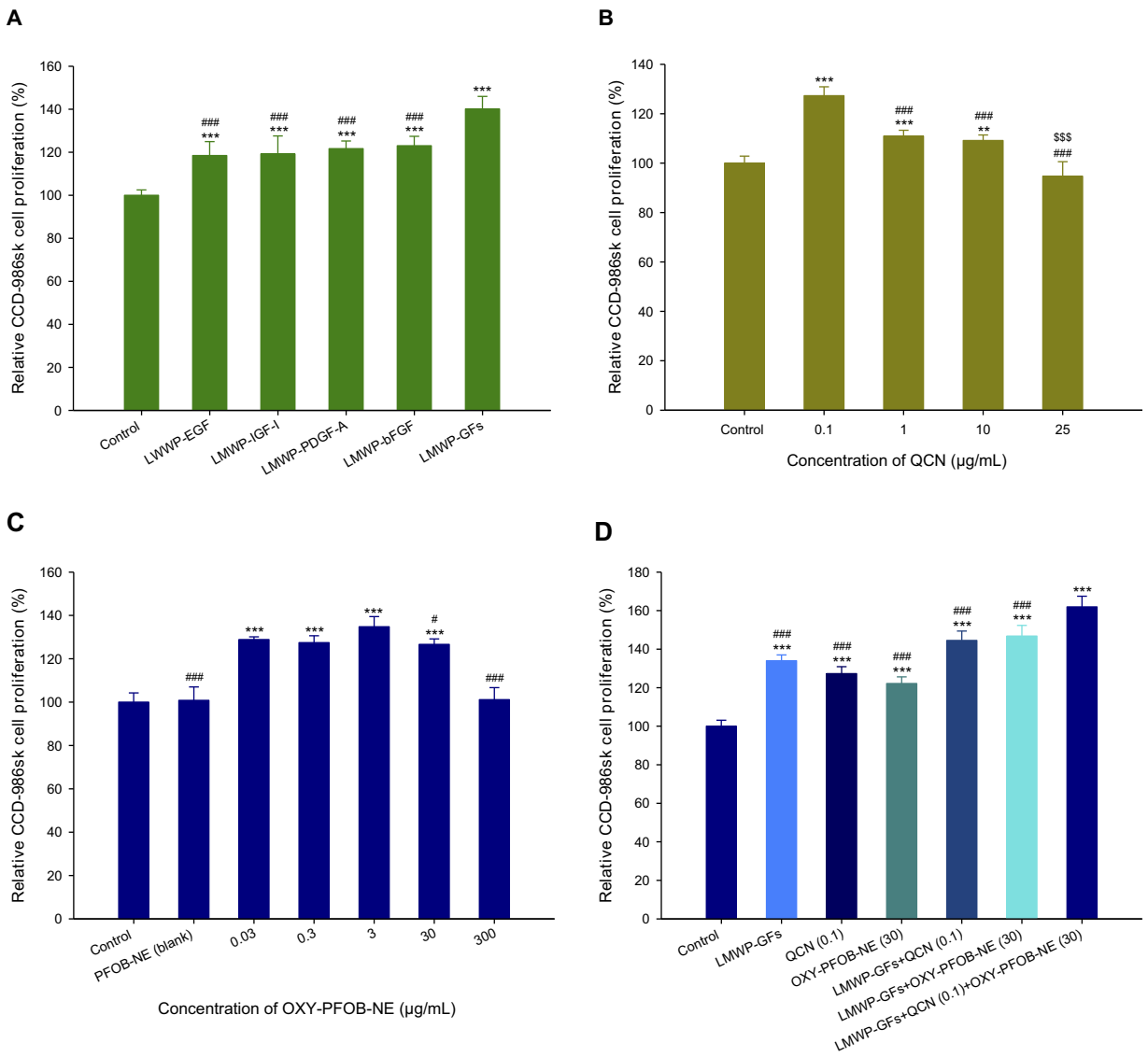

Figure S2 Fibroblast proliferation in response to treatment with LMWP-GFs, QCN-NE, and OXY-PFOB-NE. Relative fibroblast (CCD-986sk cells) proliferation after 24 h incubation with either (**A**) LMWP-GFs (***P<0.001 compared to the control group; ###P<0.001 compared to LMWP-GFs), (**B**) QCN (**P<0.01, ***P<0.001 compared to the control group; ###P<0.001 compared to QCN [0.1 μg/mL]; $$$$P$<0.001 compared to QCN [1 μg/mL]), (**C**) OXY-PFOB-NE (***P<0.001 compared to the control group; #P<0.05, ###P<0.001 compared to OXY-PFOB-NE [3 μg/mL]) alone, or (**D**) all combined. ***P<0.001 compared to the control group. ###P<0.001 compared to all LMWP-GFs, QCN, and OXY-PFOB-NE combined (LMWP-EGF [500 ng/mL] + LMWP-IGF-I [500 ng/mL] + LMWP-PDGF-A [10 ng/mL] + LMWP-bFGF [10 ng/mL] + QCN [0.1 μg/mL] + OXY-PFOB-NE [30 μg/mL]).

Notes: Cell viability was measured using WST-1 and the growth of CCD-986sk cells compared to the control group. All data are expressed as mean ± standard deviation (n=6).

Abbreviations: LMWP, low-molecular-weight protamine; GFs, growth factors; LMWP-GFs, LMWP-fused GFs; EGF, epidermal growth factor; IGF-I, insulin-like growth factor-I; PDGF-A, platelet-derived growth factor-A; bFGF, basic fibroblast growth factor; LMWP-EGF, LMWP-fused EGF; LMWP-IGF-I, LMWP-fused IGF-I; LMWP-PDGF-A, LMWP-fused PDGF-A; LMWP-bFGF, LMWP-fused bFGF; QCN, quercetin; PFOB, 1-bromoperfluorooctane; NE, nanoemulsion; OXY-PFOB-NE, oxygen-carrying PFOB-loaded NE.

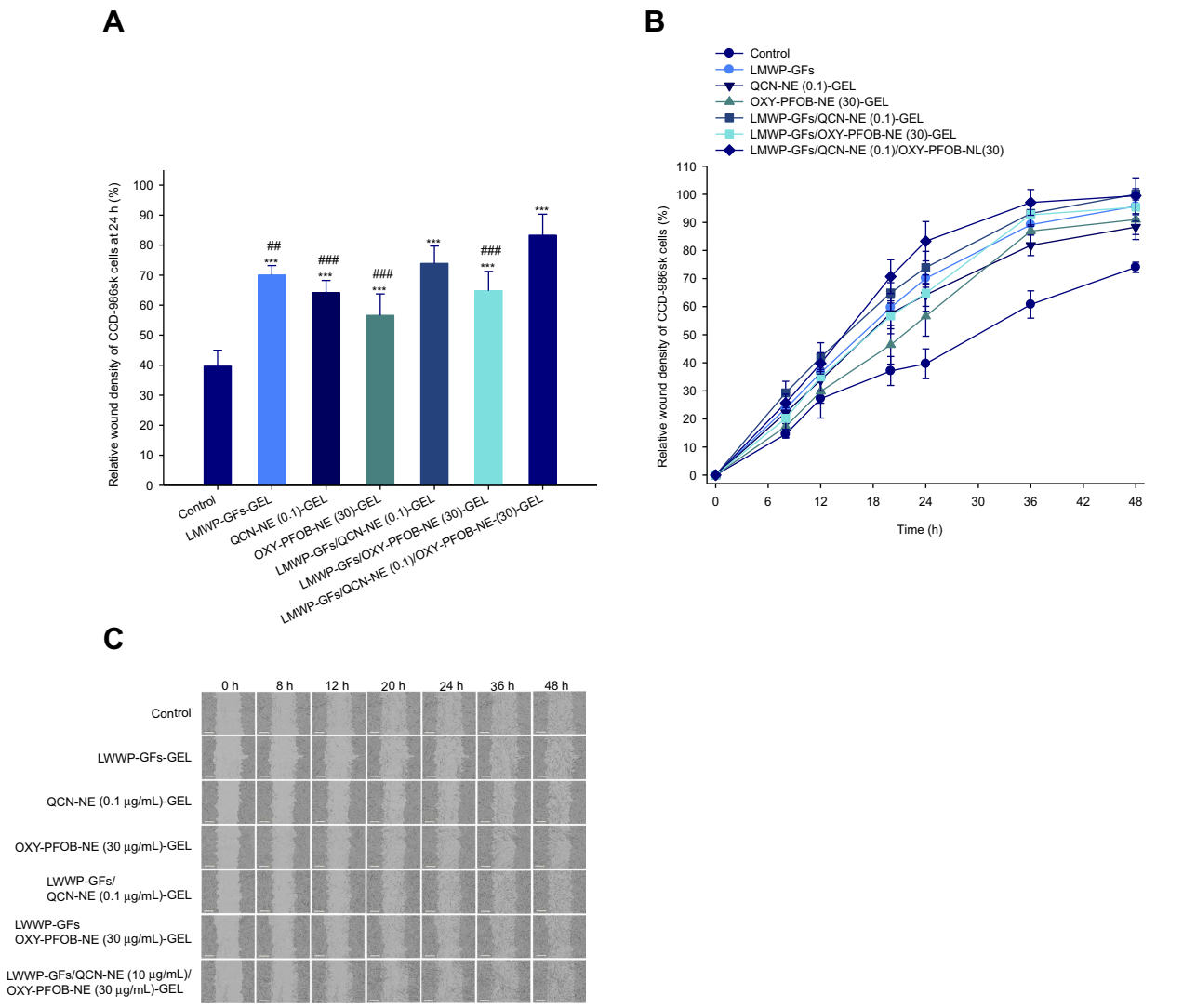

Figure S3 In vitro scratch-wound healing in fibroblasts following treatment with LMWP-GFs, QCN-NE, and OXY-PFOB-NE. (**A**) Relative scratch-wound recovery of CCD-986sk cells at 24 h. (**B**) Time-course showing relative scratch-wound recovery. (**C**) Representative microscopic images of CCD-986sk-cell scratch-wounds at 0, 8, 12, 20, 24, 36, and 48 h after incubation with serum-free medium (control) or Carbopol hydrogel containing either LMWP-GFs, QCN-NE, OXY-PFOB-NE alone, or all combined.

Notes: All data are expressed as mean ± standard deviation (n=6). ***P<0.001 compared to the control group. $^{\#\#}P$<0.01, $^{\#\#\#}P$<0.001 compared to all LMWP-GFs, QCN-NE and OXY-PFOB-NE combined (LMWP-EGF [500 ng/mL] + LMWP-IGF-I [500 ng/mL] + LMWP-PDGF-A [10 ng/mL] + LMWP-bFGF [10 ng/mL] + QCN-NE [0.1 μg/mL QCN] + OXY-PFOB-NE [30 μg/mL]). The scale bar in (C) equals 300 μm.

Abbreviations: LMWP, low-molecular-weight protamine; GFs, growth factors; LMWP-GFs, LMWP-fused GFs; EGF, epidermal growth factor; IGF-I, insulin-like growth factor-I; PDGF-A, platelet-derived growth factor-A; bFGF, basic fibroblast growth factor; LMWP-EGF, LMWP-fused EGF; LMWP-IGF-I, LMWP-fused IGF-I; LMWP-PDGF-A, LMWP-fused PDGF-A; LMWP-bFGF, LMWP-fused bFGF; QCN, quercetin; NE, nanoemulsion; QCN-NE, QCN-loaded NE; PFOB, 1-bromoperfluorooctane; OXY-PFOB-NE, oxygen-carrying PFOB-loaded NE.